Weierstraß-Institut
für Angewandte Analysis und Stochastik

Leibniz-Institut im Forschungsverbund Berlin e. V.

Preprint ISSN 2198-5855

Modeling of porous battery electrodes with multiple phase transitions – Part I: Modeling and homogenization

Martin Heida, Manuel Landstorfer

submitted: December 19, 2025

Weierstrass Institute
Anton-Wilhelm-Amo Str. 39
10117 Berlin
Germany
E-Mail: Martin.Heida@wias-berlin.de
Manuel.Landstorfer@wias-berlin.de

No. 3251
Berlin 2025

2020 *Mathematics Subject Classification.* 78A57, 35Q92, 35B27, 78M40, 80A22.

Key words and phrases. Battery, homogenization, two-scale convergence, porous electrode, non-equilibrium thermodynamics, phase separation.

M. L. acknowledges funding by the Deutsche Forschungsgemeinschaft (DFG, German Research Foundation) under Germany's Excellence Strategy – The Berlin Mathematics Research Center MATH+ (EXC-2046/1, project ID: 390685689) in project PaA-2 and M. H. by the DFG through SFB 1114 - Scaling Cascades in Complex System (project ID: 235221301) in project B09.

Edited by
Weierstraß-Institut für Angewandte Analysis und Stochastik (WIAS)
Leibniz-Institut im Forschungsverbund Berlin e. V.
Anton-Wilhelm-Amo-Straße 39
10117 Berlin
Germany

Fax: +49 30 20372-303
E-Mail: preprint@wias-berlin.de
World Wide Web: http://www.wias-berlin.de/

Modeling of porous battery electrodes with multiple phase transitions – Part I: Modeling and homogenization

Martin Heida, Manuel Landstorfer

Abstract

We derive a thermodynamically consistent multiscale model for a porous intercalation battery in a half-cell configuration. Starting from microscopically resolved balance equations, the model rigorously couples cation and anion transport in the electrolyte with electron transport and solid-state diffusion in the active material through intercalation reactions. The derivation is based on non-equilibrium thermodynamics and periodic homogenization.

The central novelty of this work lies in the systematic incorporation of multi-well free energy functions for intercalated cations into a homogenized DFN-type porous-electrode framework. This modeling choice leads to non-monotonic chemical potentials and enables a macroscopic description of phase separation and multiple phase transitions within the electrode. While multi-well free energies are well established at the particle scale, their integration into homogenized porous-electrode models has so far been lacking. By extending the homogenization framework to include Cahn–Hilliard-type regularizations, phase-transition effects are retained at the electrode level.

The resulting model exhibits an intrinsically coupled 3D+3D structure, in which macroscopic transport in the electrolyte is coupled to fully resolved microscopic diffusion within active particles. This coupling naturally induces memory effects and time lags in the macroscopic voltage response, which cannot be captured by reduced single-scale models. Although the microscopic dynamics possess an underlying gradient-flow structure, we adopt a formal asymptotic approach to obtain a tractable DFN-type model suitable for practical simulations.

This paper constitutes Part I of a three-part series and is devoted to the systematic derivation and mathematical formulation of the model. Numerical analysis, discretization strategies, simulation studies of transient cycling behavior, and experimental validation are deferred to Parts II and III. Part II focuses on finite C-rates, while Part III addresses open-circuit voltage conditions, where the predictive capabilities of the framework are investigated in detail.

DOI 10.20347/WIAS.PREPRINT.3251 Berlin 2025

1 Introduction

In this work, we derive a coupled system of balance equations describing a porous intercalation battery in a half-cell configuration. The modeling framework is based on non-equilibrium thermodynamics and rigorously couples cation and anion transport in the electrolyte with electron transport and solid-state diffusion in the active phase through intercalation reactions. This paper constitutes *Part I of a three-part series* and is devoted to the systematic derivation and mathematical formulation of the resulting multi-scale model.

The key novelty of this work lies in the consistent incorporation of multi-well free energy functions for intercalated cations into a homogenized porous-electrode model. This modeling choice gives rise to non-monotonic chemical potential functions with respect to the mole fraction, which constitute the fundamental driving mechanism for phase separation in lithium-ion batteries [16, 18, 17, 2, 12]. While such free energy formulations are well established at the particle scale, their systematic integration into DFN-type porous-electrode models via homogenization has, to the best of our knowledge, not been carried out so far. As a result, we obtain a homogenized modeling framework that naturally captures multiple phase transitions at the electrode level.

Homogenized models for porous intercalation electrodes are widely used in both science and industry to simulate the charge and discharge behavior of lithium-ion batteries, as they retain the dominant micro-structural effects while remaining computationally efficient. The classical DFN model introduced by Newman *et al.* [31, 40, 45, 30, 29] established the standard paradigm for lithium-ion battery modeling without explicit resolution of the porous microstructure. These DFN-type models, traditionally derived using the method of volume averaging [46], typically rely on monotone chemical potentials and therefore cannot represent phase separation phenomena within the active material.

More recent DFN-type model derivations based on rigorous homogenization techniques [11, 6, 7, 38, 33] improve mathematical consistency but still assume single-well free energies and thus exclude phase-transition effects by construction. In contrast, the present work extends the homogenization framework itself to accommodate multi-well free energies and Cahn–Hilliard-type regularizations, thereby enabling phase separation to be retained at the macroscopic electrode scale.

The objective of this work is therefore not merely to re-derive an existing DFN-type model, but to develop a thermodynamically consistent multi-scale framework for porous intercalation electrodes that remains valid in the presence of multiple phase transitions. Starting from microscopically resolved transport equations for the electrolyte, active material, and conductive additive phases, we apply periodic homogenization to systematically derive a macroscopic PDE system. The formulation is intentionally kept in terms of general material functions, ensuring broad applicability across different electrode chemistries.

A distinguishing feature of the resulting model is its intrinsically coupled 3D+3D structure, in which macroscopic transport in the electrolyte is coupled to fully resolved microscopic diffusion within the active particles. Unlike many reduced models, the microscopic spatial coordinate cannot be eliminated, as it encodes the internal state of charge of the particles and generates a characteristic time lag in the macroscopic voltage response. This mechanism emerges naturally from the homogenization procedure and is essential for accurately capturing phase-transition dynamics.

In earlier work [27], the present authors performed a mathematically rigorous homogenization of a related but simpler intercalation model using periodic unfolding and exploiting its gradient-flow structure. While the microscopic model derived here exhibits an analogous gradient structure, pursuing a fully rigorous analysis would substantially increase technical complexity and obscure the modeling

insights. Instead, the present work deliberately adopts a formal asymptotic approach in order to derive a tractable DFN-type model suitable for practical simulations, while still preserving the underlying thermodynamic structure.

1.1 Outline

Despite its increased complexity, the homogenized model retains a dissipative gradient-flow character and can be written as a coupled system of parabolic and elliptic equations. This ensures intrinsic numerical stability and makes the framework well suited for standard finite element and finite volume discretization. Numerical analysis, discretization strategies, simulation studies, and experimental validation are deferred to Parts II and III of this series. In the present work, we focus exclusively on the model derivation.

The remainder of this paper is organized as follows. In Section 2, we introduce the general modeling principles, including the domain setup (Section 2.1), general transport equations (Section 2.2), thermodynamic principles (Section 2.3), and the electro-neutrality condition together with its implications (Section 2.4). Material models and transport equations for the electrolyte phase (Section 3.1), the active phase, and the conductive additive (Section 3.2) are then formulated, with particular emphasis on general multi-well free energy functions and interfacial free energy contributions expressed via gradient terms. The coupling of the phases through interfacial reaction boundary conditions is discussed in Section 3.4, and the resulting transport equations are summarized in Section 3.3.

In Section 4, we describe the half-cell setup, including boundary conditions and corresponding initial conditions. Appropriate scalings are introduced in Section 4.3, leading to a non-dimensioqnalized system in Section 4.3.2. Based on this formulation, the ε-problem and the associated two-scale model are introduced in Section 5, where the geometric setup and the scaling of all transport parameters with respect to ε are discussed. The multi-scale asymptotic expansion of all variables is presented in Section 5.3.

Finally, in Section 6, we perform the homogenization of a porous electrode undergoing multiple phase transitions. This includes the balance equation for charge in the solid phase (Section 6.1), the balance equations for charge and cations in the electrolyte (Section 6.2.1), and the balance equation for intercalated cations in the active phase (Section 6.3). The homogenized balance equations are summarized in Section 7.1, followed by an outlook in Section 7.2.

2 General Modeling

2.1 Domains, Definitions, and Initial Scaling

We aim to model a porous intercalation electrode Ω which consists of three distinct phases: the active particle phase $\Omega_{\mathtt{A}}$, the conductive additive phase $\Omega_{\mathtt{C}}$, and the electrolyte phase $\Omega_{\mathtt{E}}$, with $\Omega = \bigcup_{i\in\mathtt{A},\mathtt{C},\mathtt{E}} \Omega_i$. The combined active and conductive additive phases are commonly referred to as the solid phase, denoted as $\Omega_{\mathtt{S}} = \Omega_{\mathtt{A}} \cup \Omega_{\mathtt{C}}$.

The interface $\Sigma_{\mathtt{AE}} = \Omega_{\mathtt{A}} \cap \Omega_{\mathtt{E}}$ covers the actual surface of the active particle as well as the adjacent space charge layers, whereby $\Omega_{\mathtt{A}}$ and $\Omega_{\mathtt{E}}$ are electro-neutral. In 2.4 we sketch some aspects of the electro-neutrality condition and refer to [43, 35, 20] for details and the derivation based on asymptotic expansions. The electron based electrical current enters the porous electrode via a current collector,

which is connected to the solid phase $\Omega_{\mathtt{S}}$ and denoted by $\Sigma_{\mathtt{CC}} \subset \partial\Omega_{\mathtt{S}}$. The ionic electrical current enters the porous electrode over the interface $\Sigma_{\mathtt{EE}} \subset \partial\Omega_{\mathtt{E}}$, which can also be considered as electrolytic reservoir. We further formulate in section 4 conditions for the electrolytic reservoir reflecting the conditions of an electro-chemical half cell, *i.e.* contact to a metallic .

In the following, we sketch the balance equations in each phase as well as the boundary conditions that describe the intercalation reaction $\mathrm{Li}^+ + \mathrm{e}^- \rightleftharpoons \mathrm{Li}$ which occurs at the electrolyte-active phase interface $\Sigma_{\mathtt{AE}}$.

2.2 General Transport Equations

We consider each domain $\Omega_i, i = \mathtt{A}, \mathtt{C}, \mathtt{E}$ as a mixture of species $\alpha \in \mathcal{I}_i$ for which we have balance equations

$$\frac{\partial n_\alpha}{\partial t} = -\operatorname{div}\left(n_\alpha \mathbf{v} + \mathbf{J}_\alpha\right), \tag{1}$$

where $n_\alpha(\mathbf{x}, t)$ denotes the molar density, $\mathbf{v}$ the barycentric velocity of the mixture, and $\mathbf{J}_\alpha$ the molar flux of constituent α. The mass density $\rho = \sum_\alpha m_\alpha$, where m_α is the molar mass of constituent $\alpha \in \mathcal{I}$ satisfies

$$\frac{\partial \rho}{\partial t} = -\operatorname{div}\left(\rho \mathbf{v}\right), \tag{2}$$

whereby[25, 41]

$$\sum_{\alpha\in\mathcal{I}} m_\alpha \mathbf{J}_\alpha = \mathbf{0}. \tag{3}$$

Since we consider charged matter, this is accompanied with Poisson equation[21, 22]

$$-\operatorname{div}\left(\varepsilon_0(1+\chi)\nabla\varphi\right) = e_0 \sum_{\alpha\in\mathcal{I}} z_\alpha n_\alpha =: q\,, \tag{4}$$

where φ denotes the electrostatic potential, χ the dielectric susceptibility, e_0 the elementary charge, z_α the charge number, and q the charge density. The charge balance is in general

$$\frac{\partial q}{\partial t} = -\operatorname{div}\left(q\mathbf{v} + \mathbf{J}_q\right), \qquad \text{where} \qquad \mathbf{J}_q = e_0 \sum_{\alpha\in\mathcal{I}} z_\alpha \mathbf{J}_\alpha\,, \tag{5}$$

denotes the (free) charge flux.

Throughout this work, we consider mechanical equilibrium, whereby the momentum balance reads [25, 21]

$$\nabla p = -q\nabla\varphi\,, \tag{6}$$

which reflects the balance between the (electrostatic) Lorentz force and the mechanical counterforce by a gradient of the (mechanical) pressure p[32]. Further, we consider a vanishing barycentric velocity

$$\mathbf{v} = \mathbf{0}$$

[14] throughout this work and refer to [26, 42] for details on the full non-equilibrium thermodynamics of charged matter.

2.3 Chemical Potential Functions and the Second Law of Thermodynamics

The mixtures in each domain Ω_i are modeled by continuum non-equilibrium thermodynamics. We denote with $\rho\psi = \rho\psi(T, (n_\alpha)_{\alpha\in\mathcal{I}})$ the free energy density of the mixture and with

$$\mu_\alpha = \frac{\partial \rho\psi}{\partial n_\alpha} \qquad \alpha \in \mathcal{I} \tag{7}$$

the (molar) chemical potential (function) of constituent $\alpha \in \mathcal{I}$. In order to exploit the constraint

$$\sum_{\alpha\in\mathcal{I}} m_\alpha \mathbf{J}_\alpha = \mathbf{0}\,, \tag{8}$$

it is convenient to consider one species $\gamma \in \mathcal{I}$ as *reference system*, e.g. the solvent in liquid electrolyte or the lattice forming species in solids, and introduce

$$\mathcal{I}^0 = \mathcal{I} \setminus \{\gamma\}\,, \quad \text{such that} \quad \sum_{\alpha\in\mathcal{I}^0} \frac{m_\alpha}{m_\gamma}\mathbf{J}_\alpha = -\mathbf{J}_\gamma\,. \tag{9}$$

A core ingredient of non-equilibrium thermodynamics is to state necessary conditions for fluxes and reaction rates to ensure the second law of thermodynamics, i.e. a non-negative entropy production. For the molar fluxes $\mathbf{J}_\alpha$, this essentially means[1] [25, 41]

$$\mathbf{J}_\alpha = -\sum_{\beta\in\mathcal{I}^0} \frac{1}{k_{\mathrm{B}}T}\mathbf{M}_{\alpha\beta}\nabla\tilde{\mu}_\beta \qquad \tilde{\mu}_\beta := \mu_\beta - \frac{m_\beta}{m_\gamma}\mu_\gamma + e_0 z_\beta \varphi\,, \tag{10}$$

with a symmetric, positive semi-definite matrix $\mathbf{M} = (\mathbf{M}_{\alpha\beta})_{\alpha\in\mathcal{I}^0,\beta\in\mathcal{I}^0}$, whereby the entropy production due to (diffusional) fluxes is [25, 41]

$$\sigma^{\mathbf{J}} := -\sum_{\alpha\in\mathcal{I}^0} \frac{1}{T}\mathbf{J}_\alpha^T(\nabla\tilde{\mu}_\alpha) = \sum_{\alpha\in\mathcal{I}^0}\sum_{\beta\in\mathcal{I}^0} (\nabla\tilde{\mu}_\beta)^T \frac{\mathbf{M}_{\alpha\beta}}{k_{\mathrm{B}}T}(\nabla\tilde{\mu}_\alpha) \geq 0\,. \tag{11}$$

For a chemical reaction $R_k (k = 1, \ldots, N_R)$, i.e.

$$\sum_\alpha \nu'_{\alpha,k}\mathrm{A}_\alpha \rightleftharpoons \sum_\alpha \nu''_{\alpha,k}\mathrm{A}_\alpha\,, \tag{12}$$

where

$$\lambda_k := -\frac{1}{k_{\mathrm{B}}T}\sum_\alpha \nu_{\alpha,k}\mu_\alpha \quad \text{with} \quad \nu_{\alpha,k} := \nu''_{\alpha,k} - \nu'_{\alpha,k} \tag{13}$$

is the affinity[2] of the reaction R_k , the entropy production due to chemical reactions is [25, 41, 22]

$$\sigma^R = \sum_{k=1}^{N_R} \lambda_k \cdot R_k\,, \tag{14}$$

Choosing hence [20, 35, 34]

$$R_k = L_k \cdot f_{\mathtt{BV}}(\lambda_k) \quad \text{with} \quad f_{\mathtt{BV}}(\lambda) := \mathrm{e}^{\alpha\lambda} - \mathrm{e}^{-(1-\alpha)\lambda}\,, \tag{15}$$

ensures $\sigma^R \geq 0$, i.e. a non-negative entropy production. We call $f_{\mathtt{BV}}$ a Butler-Volmer-type relation with the charge transfer coefficient α and emphasize that $f_{\mathtt{BV}}(z)|_{z>0} > 0$. Note, however, that among the literature [40, 1, 4, 10, 5, 23, 39, 3, 19, 30, 11, 29] the term *Butler-Volmer*-reaction or -type is not uniformly used[34].

[1] Note that we consider only the isothermal case here

[2] We follow here the IUPAC definition of reaction affinity. Note, however, that among the literature also definitions with a $+$ sign are found.

2.4 Electro-neutrality condition

A common and very useful simplification of the coupled equation system is the (strong) electro-neutrality condition

$$q = \sum_{\alpha \in \mathcal{I}} e_0 z_\alpha n_\alpha = 0 \,. \tag{16}$$

which holds outside of spatially small space charge layers at electrode-electrolyte interfaces. The electro-neutrality condition can be derived through an asymptotic expansion of the balance equations within the space charge layers as well as matching conditions. Here, we summarize the key conclusions and refer to [43, 32, 35, 19, 20, 34] for further details on the modeling, validation, and asymptotic derivation.

Besides the condition $q = 0$, a key feature of the electro-neutrality condition is the continuity of the electrochemical potential $\mu_\alpha + e_0 z_\alpha \varphi$ across doubles layers (in equilibrium). This allows to *trace back* the evaluation of a quantity right at the surface to a point outside of the space charge layer, along with the potential drop across the space charge layer. This is of particular importance for surface reactions which occur at the surface of an electrode (c.f. section 3.3).

If $\underset{s}{\mu_\alpha}$ denotes the surface chemical potential of a constituent A_α and $\underset{s}{\varphi}$ the electro-static potential at the surface of Σ_{ij}, the continuity of the electrochemical potential allows us to write

$$\underset{s}{\mu_\alpha} = \mu_\alpha|^k_{\Sigma_{ij}} + e_0 z_\alpha (\varphi|^k_{\Sigma_{ij}} - \underset{s}{\varphi}) \,. \tag{17}$$

where $k \in \{i, j\}$ indicates at which side of the interface we evaluate the volume quantities. Note that $\mu_\alpha|^k_{\Sigma_{ij}}$ and $\varphi|^k_{\Sigma_{ij}}$ correspond to the (volumetric) chemical potential and electrostatic potential outside of the space charge layer. The conditions (17) allows us in section 3.3 to trace back the surface chemical potential towards points outside of the space charge layer for intercalation reactions.

If it is clear from the context which Σ_{ij} is meant, we drop the index $_{ij}$ and emphasize by ^{k} only at what side of the interface the evaluation occurs, and we denote with φ_k the electrostatic potential in Ω_k. If a constituent is only present in one phase, e.g. E_C only in $\Omega_{\mathtt{E}}$, we drop the index ^{k}, e.g. $\mu_{\mathrm{E}_C}|^{\mathtt{E}}_{\Sigma_{\mathtt{AE}}} = \mu_{\mathrm{E}_C}|_\Sigma$.

3 Material Models

In section 3.1 we will state material models for an incompressible, liquid electrolyte which is subject to solvation effects. We state the corresponding transport parameters, including cross diffusion effects, and exploit the charge neutrality of the electrolyte which yields a full set of balance equations for the electrolyte phase. In 3.2 we state material models for the intercalated cations in the active phase and introduce multi-well free energy functions, yielding non-monotonic chemical potential functions. Further, we state the electron transport in the solid phase, and discuss the corresponding transport parameter. In 3.3 we state the reaction rate model for the intercalation reaction and show how this reaction couples the all previously stated balance equations.

3.1 Electrolyte

For the electrolyte, we adopt an incompressible liquid electrolyte model [14, 32, 21], which incorporates solvation effects. We consider thus electrolyte in the domain Ω^{E} as a mixture $\mathcal{I}_{\mathrm{E}} = \{\mathrm{E}_S, \mathrm{E}_A, \mathrm{E}_C\}$ of solvent E_S, anions E_A and cations E_C with their corresponding molar densities n_α. As reference species (c.f. section 2.2) we consider the solvent, i.e. $\gamma = \mathrm{E}_S$, whereby $\mathcal{I}^0_{\mathrm{E}} = \{\mathrm{E}_A, \mathrm{E}_C\}$. Each ion $\alpha \in \mathcal{I}^0_{\mathrm{E}}$ is assumed to bind κ_α solvent molecules, which has various impacts on the mixture theory, and we refer to [32] for detailed discussions.

The chemical potential functions of the electrolyte species are [32]

$$\mu_\alpha = g_\alpha + k_{\mathrm{B}} T \ln(y_\alpha) + v_\alpha p \qquad \alpha \in \mathcal{I}_{\mathrm{E}}, \tag{18}$$

where g_α is the (constant) molar Gibbs energy, k_{B} the Boltzmann constant, T the temperature, y_α the mole fraction, satisfying

$$y_\alpha = \frac{n_\alpha}{n_{\mathrm{E,tot}}}, \quad n_{\mathrm{E,tot}} = n_{\mathrm{E}_S} + n_{\mathrm{E}_A} + n_{\mathrm{E}_C}, \quad \sum_\alpha y_\alpha = 1\,, \tag{19}$$

and v_α being the partial molar volume.

The second term of the chemical potential corresponds to the entropy of mixing [14], while the third term is the mechanical contribution due to the incompressibility. Note that v_α captures also the solvation effect, whereby in general $v_{\mathrm{E}_A,\mathrm{E}_C} > v_S$.

The incompressibility entails the constraint [14]

$$\sum_{\alpha \in \mathcal{I}_{\mathrm{E}}} n_\alpha v_\alpha = 1\,, \tag{20}$$

whereby we can write

$$n_\alpha = \frac{y_\alpha}{\sum_{\beta \in \mathcal{I}_{\mathrm{E}}} v_\beta y_\beta}\,, \tag{21}$$

as well as the electrolyte pressure p_{E} as an independent variable. We assume throughout this work that

$$\frac{m_\alpha}{m_{\mathrm{E}_S}} = \frac{v_\alpha}{v_{\mathrm{E}_S}}, \quad \alpha \in \{\mathrm{E}_A, \mathrm{E}_C\}\,, \tag{22}$$

whereby not only mass, but also volume is conserved during solvation reactions. The molar mass of a solvated ion is $m_\alpha = \hat{m}_\alpha + \kappa_\alpha m_{\mathrm{E}_S}$, where $\hat{m}_\alpha$ is the molar mass of the central ion, κ_α the solvation number, and m_{E_S} the molar mass of the solvent. Hence

$$\frac{m_\alpha}{m_{\mathrm{E}_S}} = \frac{\hat{m}_\alpha}{m_{\mathrm{E}_S}} + \kappa_\alpha, \quad v_\alpha = \frac{\hat{m}_\alpha}{m_{\mathrm{E}_S}} v_{\mathrm{E}_S} + \kappa_\alpha v_{\mathrm{E}_S}\,. \tag{23}$$

If $m_{\mathrm{E}_S} \gg \hat{m}_\alpha$, we can approximate $v_\alpha \approx \kappa_\alpha v_{\mathrm{E}_S}$, which we assume to be the case for the rest of this work, leading to

$$\kappa_\alpha = \frac{m_\alpha}{m_{\mathrm{E}_S}} = \frac{v_\alpha}{v_{\mathrm{E}_S}}, \quad \alpha \in \{\mathrm{E}_A, \mathrm{E}_C\}\,, \tag{24}$$

For an electrolyte consisting of three species, i.e. anions, cations and solvent, we have two independent ion fluxes ($\alpha \in \{\mathrm{E}_A, \mathrm{E}_C\}$),

$$\mathbf{J}_{\mathrm{E}_C} = -\mathbf{M}^{\mathrm{E}}_{C,A}\frac{1}{k_{\mathrm{B}}T}\nabla\tilde{\mu}_{\mathrm{E}_A} - \mathbf{M}^{\mathrm{E}}_{C,C}\frac{1}{k_{\mathrm{B}}T}\nabla\tilde{\mu}_{\mathrm{E}_C} \tag{25}$$

$$\mathbf{J}_{\mathrm{E}_A} = -\mathbf{M}^{\mathrm{E}}_{A,A}\frac{1}{k_{\mathrm{B}}T}\nabla\tilde{\mu}_{\mathrm{E}_A} - \mathbf{M}^{\mathrm{E}}_{A,C}\frac{1}{k_{\mathrm{B}}T}\nabla\tilde{\mu}_{\mathrm{E}_C}\ , \tag{26}$$

satisfying

$$\frac{\partial n_{\mathrm{E}_C}}{\partial t} = -\operatorname{div}\mathbf{J}_{\mathrm{E}_C}\ , \qquad \frac{\partial n_{\mathrm{E}_A}}{\partial t} = -\operatorname{div}\mathbf{J}_{\mathrm{E}_A}\ , \tag{27}$$

where for $\alpha \in \mathcal{I}^0_{\mathrm{E}}$ according to (10) and (24)

$$\tilde{\mu}_\alpha := \mu_\alpha - \kappa_\alpha\mu_{\mathrm{E}_S} + e_0 z_\alpha\varphi_{\mathrm{E}}\ , \tag{28}$$

is the *effective* electro-chemical potential of the ion in its solvated state. The symmetric structure of (25) and (27) is of great importance for the spatial homogenization of the electrolyte domain, i.e. the well-definedness of the cell-problem and the effective model.

3.1.1 Electrolyte transport equations in terms of mobilities

The mobilities $\mathbf{M}_{\alpha,\beta}$, where $(\mathbf{M}_{\alpha,\beta})_{\alpha,\beta}$ is symmetric and positive semi-definite[25], are connected to the (constant) diffusion coefficients $D_{\alpha,\alpha}$ and the friction $F_{A,C} = F_{C,A}$via

$$\mathbf{M}^{\mathrm{E}}_{A,A} = n_{\mathrm{E}_A}D_{A,A}, \quad \mathbf{M}^{\mathrm{E}}_{C,C} = n_{\mathrm{E}_C}D_{C,C}, \quad \mathbf{M}^{\mathrm{E}}_{A,C} = \frac{y_{\mathrm{E}_C}y_{\mathrm{E}_A}}{n_{\mathrm{E,tot}}}F_{A,C}. \tag{29}$$

Note that for the simpler Nernst–Planck flux approach [21, 44] the friction coefficients $F_{A,C}$ vanish, yielding

$$\mathbf{J}_\alpha = D_{\alpha,\alpha}\frac{n_\alpha}{k_{\mathrm{B}}T}\nabla\tilde{\mu}_\alpha\ , \quad \alpha = \mathrm{E}_A, \mathrm{E}_C, \tag{30}$$

with constant diffusion coefficients $D_{\alpha,\alpha}$.

The electrolyte is thus in general described by the variables $(y_{\mathrm{E}_C}, y_{\mathrm{E}_A}, p_{\mathrm{E}}, \varphi_{\mathrm{E}})$, where p_{E} denotes the pressure and φ_{E} the electrostatic potential in the electrolyte, satisfying the equation system (25) and (27), together with the chemical potential functions (18), the constraints (20) and (19), the definition (28) and the stationary Poisson-momentum balance equations

$$-\operatorname{div}(\varepsilon_0(1+\chi_{\mathrm{E}})\nabla\varphi = q_{\mathrm{E}}, \qquad -\nabla p_{\mathrm{E}} = q_{\mathrm{E}}\nabla\varphi_{\mathrm{E}}\ , \qquad q_{\mathrm{E}} = e_0\sum_{\alpha\in\mathcal{I}^0_E} z_\alpha n_\alpha\ . \tag{31}$$

We consider the for the electrolyte the (strong) electro-neutrality condition (16)

$$q_{\mathrm{E}} = \sum_\alpha e_0 z_\alpha n_\alpha = 0 \quad \Leftrightarrow \qquad y_{\mathrm{E}_C} = \frac{z_{\mathrm{E}_A}}{z_{\mathrm{E}_C}}y_{\mathrm{E}_A} =: y_{\mathrm{E}}\ , \tag{32}$$

which holds outside of the thin space charge layers at electrode-electrolyte interfaces.

For the following, we consider a mono-valent salt, whereby $z_{\mathrm{E}_A} = -z_{\mathrm{E}_C}$ and identical solvation numbers of cations and anions, i.e. $\kappa_{\mathrm{E}_A} = \kappa_{\mathrm{E}_C} =: \kappa_{\mathrm{E}}$. Note, however, that these restrictions are in general necessary, but reflect the major use of mono-valent salts in intercalation batteries.

By the electro-neutrality condition, the set of variables $(y_{\mathrm{E}_C}, y_{\mathrm{E}_A}, p_{\mathrm{E}}, \varphi_{\mathrm{E}})$ actually reduces to $(y_{\mathrm{E}}, \varphi_{\mathrm{E}})$, since the momentum balance (6) entails $p_{\mathrm{E}} = \text{const.}$ for $q_{\mathrm{E}} = 0$. The Poisson-equation (4) degenerates outside of the space charge layers and the charge balance (5) actually serves to determine φ_{E}.

Note, however, that from a thermodynamic perspective, $\tilde{\mu}_{\mathrm{E}_C}$ and $\tilde{\mu}_{\mathrm{E}_A}$ are convenient (and equivalent) variables, replacing y_{E_C} and y_{E_A}, which satisfy the variable transformations

$$\frac{1}{2}(\tilde{\mu}_{\mathrm{E}_C} - \tilde{\mu}_{\mathrm{E}_A}) = e_0\varphi_{\mathrm{E}} + \underbrace{\frac{1}{2}(g_{\mathrm{E}_C} - g_{\mathrm{E}_A})}_{=\text{const.}} \tag{33}$$

$$\frac{1}{2}(\tilde{\mu}_{\mathrm{E}_C} + \tilde{\mu}_{\mathrm{E}_A}) = k_{\mathrm{B}}T\, f_{\mathrm{E}}(y_{\mathrm{E}}) + \underbrace{\frac{1}{2}(g_{\mathrm{E}_A} + g_{\mathrm{E}_C} - 2\kappa_{\mathrm{E}} g_{\mathrm{E}_S})}_{=\text{const.}} \tag{34}$$

$$f_{\mathrm{E}} := \ln(y_{\mathrm{E}}) - \kappa_{\mathrm{E}} \ln(1 - 2y_{\mathrm{E}}) \tag{35}$$

Throughout this work, we will make use of this variable transformation since the representation (25) of the ionic fluxes employs the very useful positive definiteness of the mobility matrices $(\mathbf{M}_{\alpha,\beta})_{\alpha,\beta}$.

3.1.2 Electrolyte transport in terms of transference numbers, conductivities and diffusion coefficients

The total number density $n_{\mathrm{E,tot}} = n_{\mathrm{E}_S} + n_{\mathrm{E}_C} + n_{\mathrm{E}_A}$ and the electrolyte concentration n_{E_C} can be expressed as functions of y_{E}, using Eq. (20), as follows:

$$n_{\mathrm{E,tot}} = n_{\mathrm{E}_S} \cdot \frac{1}{1 + 2(\kappa_{\mathrm{E}} - 1)y_{\mathrm{E}}} = n_{\mathrm{E,tot}}(y_{\mathrm{E}}), \tag{36}$$

$$n_{\mathrm{E}_C} = n_{\mathrm{E}_S} \frac{y_{\mathrm{E}}}{1 + 2(\kappa_{\mathrm{E}} - 1)y_{\mathrm{E}}} = n_{\mathrm{E}_C}(y_{\mathrm{E}}). \tag{37}$$

Note, however, that $\tilde{\mu}_{\mathrm{E}_C}$ and $\tilde{\mu}_{\mathrm{E}_A}$ can yet be considered as independent variables, where φ_{E} is determined via (33) and y_{E_C} via (34).

Since the electro-neutrality ($y_{\mathrm{E}_A} = y_{\mathrm{E}_C}$) implies $\nabla\mu_{\mathrm{E}_A} = \nabla\mu_{\mathrm{E}_C}$, we can compute

$$\nabla(\mu_{\mathrm{E}_C} - \kappa_{\mathrm{E}_C}\mu_{\mathrm{E}_S}) = k_{\mathrm{B}}T \frac{1}{y_{\mathrm{E}_C}} \Gamma_{\mathrm{E}} \cdot \nabla y_{\mathrm{E}_C} \quad \text{with} \quad \Gamma_{\mathrm{E}} := 1 + \kappa_{\mathrm{E}_C} \frac{2y_{\mathrm{E}_C}}{(1 - 2y_{\mathrm{E}_S})} = y_{\mathrm{E}} \cdot \frac{\partial f_{\mathrm{E}}}{\partial y_{\mathrm{E}}}\,, \tag{38}$$

and call Γ_{E} thermodynamic factor. Hence we obtain the equivalent representations of the ion fluxes

$$\mathbf{J}_{\mathrm{E}_C} = -\mathbf{M}^{\mathrm{E}}_{C,A} \frac{1}{k_{\mathrm{B}}T} \nabla\tilde{\mu}_{\mathrm{E}_A} - \mathbf{M}^{\mathrm{E}}_{C,C} \frac{1}{k_{\mathrm{B}}T} \nabla\tilde{\mu}_{\mathrm{E}_C} \tag{39}$$

$$= -(\mathbf{D}^{\mathrm{E}}_{C,C} + \mathbf{F}^{\mathrm{E}}_{C,A}) n_{\mathrm{E,tot}} \Gamma_{\mathrm{E}} \nabla y_{\mathrm{E}} - n_{\mathrm{E,tot}} y_{\mathrm{E}_C} (\mathbf{D}^{\mathrm{E}}_{C,C} - \mathbf{F}^{\mathrm{E}}_{C,A}) \frac{e_0}{k_{\mathrm{B}}T} \nabla\varphi_{\mathrm{E}} \tag{40}$$

$$\mathbf{J}_{\mathrm{E}_A} = -\mathbf{M}^{\mathrm{E}}_{A,A} \frac{1}{k_{\mathrm{B}}T} \nabla\tilde{\mu}_{\mathrm{E}_A} - \mathbf{M}^{\mathrm{E}}_{A,C} \frac{1}{k_{\mathrm{B}}T} \nabla\tilde{\mu}_{\mathrm{E}_C} \tag{41}$$

$$= -(\mathbf{D}^{\mathrm{E}}_{A,A} + \mathbf{F}^{\mathrm{E}}_{C,A}) n_{\mathrm{E,tot}} \Gamma_{\mathrm{E}} \nabla y_{\mathrm{E}} + n_{\mathrm{E,tot}} y_{\mathrm{E}_C} (\mathbf{D}^{\mathrm{E}}_{A,A} - \mathbf{F}^{\mathrm{E}}_{C,A}) \frac{e_0}{k_{\mathrm{B}}T} \nabla\varphi_{\mathrm{E}}, \tag{42}$$

The electrolytic charge density $q^{\mathrm{E}} = e_0(z_{\mathrm{E}_A} n_{\mathrm{E}_A} + z_{\mathrm{E}_C} n_{\mathrm{E}_C})$ and charge flux

$$\mathbf{J}_{\mathrm{E}_q} = e_0(z_{\mathrm{E}_A} \mathbf{J}_{\mathrm{E}_A} + z_{\mathrm{E}_C} \mathbf{J}_{\mathrm{E}_C}) \tag{43}$$

satisfy the charge balance eq. (5), *i.e.*

$$0 = -\operatorname{div} \mathbf{J}_{\mathrm{E}_q} \,, \tag{44}$$

which is stationary due to the electro-neutrality condition $q^{\mathrm{E}} = 0$. It is hence a common and convenient approach to replace the anion balance equation by the charge balance, where the charge flux writes as

$$\begin{aligned} \mathbf{J}_{\mathrm{E}_q} =& -e_0(\mathbf{D}^{\mathrm{E}}_{C,C} - \mathbf{D}^{\mathrm{E}}_{A,A}) n_{\mathrm{E,tot}} \Gamma_{\mathrm{E}} \nabla y_{\mathrm{E}_C} - \frac{e_0^2}{k_{\mathrm{B}} T} n_{\mathrm{E,tot}} y_{\mathrm{E}_C} \big(\mathbf{D}^{\mathrm{E}}_{C,C} + \mathbf{D}^{\mathrm{E}}_{A,A} - 2\mathbf{F}^{\mathrm{E}}_{A,C}\big) \nabla \varphi_{\mathrm{E}} && (45)\\ =& -\mathbf{S}_{\mathrm{E}} \cdot n_{\mathrm{E,tot}} \Gamma_{\mathrm{E}} \nabla y_{\mathrm{E}} - n_{\mathrm{E,tot}} y_{\mathrm{E}} \mathbf{\Lambda}_{\mathrm{E}} \nabla \varphi_{\mathrm{E}}. && (46) \end{aligned}$$

and substitute $\nabla \varphi_{\mathrm{E}}$ in the cation balance by the charge flux $\mathbf{J}_{\mathrm{E}_q}$, which yields the representation

$$\begin{aligned} \mathbf{J}_{\mathrm{E}_C} =& -\mathbf{D}_{\mathrm{E}} n_{\mathrm{E,tot}} \Gamma_{\mathrm{E}} \nabla y_{\mathrm{E}_C} + \frac{1}{z_C e_0} \mathbf{t}_{\mathrm{E}_C} \mathbf{J}_{\mathrm{E}_q} && (47)\\ =& -\underbrace{(\mathbf{D}_{\mathrm{E}} + \mathbf{t}_{\mathrm{E}_C} \frac{\mathbf{S}_{\mathrm{E}}}{e_0}) n_{\mathrm{E,tot}} \Gamma_{\mathrm{E}}}_{=:\mathbf{D}^y_{\mathrm{E}}} \nabla y_{\mathrm{E}} - \underbrace{n_{\mathrm{E,tot}} y_{\mathrm{E}} \frac{1}{e_0} \mathbf{t}_{\mathrm{E}_C} \mathbf{\Lambda}_{\mathrm{E}}}_{=:\mathbf{D}^{\varphi}_{\mathrm{E}}} \nabla \varphi_{\mathrm{E}}, && (48) \end{aligned}$$

with the set of transport parameters

$$\mathbf{\Lambda}_{\mathrm{E}} := \frac{e_0^2}{k_{\mathrm{B}} T} \left(\mathbf{D}^{\mathrm{E}}_{A,A} + \mathbf{D}^{\mathrm{E}}_{C,C} - 2\mathbf{F}^{\mathrm{E}}_{A,C}\right), \tag{49}$$

$$\mathbf{t}_{\mathrm{E}_C} := \frac{\mathbf{D}^{\mathrm{E}}_{C,C} - \mathbf{F}^{\mathrm{E}}_{C,A}}{\mathbf{D}^{\mathrm{E}}_{C,C} + \mathbf{D}^{\mathrm{E}}_{A,A} - 2\mathbf{F}^{\mathrm{E}}_{A,C}}, \tag{50}$$

$$\mathbf{D}_{\mathrm{E}} := \frac{2(\mathbf{D}^{\mathrm{E}}_{A,A} \mathbf{D}^{\mathrm{E}}_{C,C} - \mathbf{F}^2_{AC})}{\mathbf{D}^{\mathrm{E}}_{C,C} + \mathbf{D}^{\mathrm{E}}_{A,A} - 2\mathbf{F}^{\mathrm{E}}_{A,C}}, \tag{51}$$

$$\mathbf{S}_{\mathrm{E}} := e_0(\mathbf{D}^{\mathrm{E}}_{C,C} - \mathbf{D}^{\mathrm{E}}_{A,A}), \tag{52}$$

satisfying the constraint

$$\frac{k_{\mathrm{B}} T}{e_0}(2\mathbf{t}_{\mathrm{E}_C} - 1) = \frac{\mathbf{S}_{\mathrm{E}}}{\mathbf{\Lambda}_{\mathrm{E}}} \,. \tag{53}$$

A major simplification of this representations arises, **when** $\mathbf{t}_{\mathrm{E}_C} =$ const. w.r.t. y_{E}, which, for instance, occurs in simple Nernst-Planck type fluxes without cross diffusion. Then,

$$-\operatorname{div} \mathbf{J}_{\mathrm{E}_C} = \operatorname{div} (\mathbf{D}_{\mathrm{E}} n_{\mathrm{E,tot}} \Gamma_{\mathrm{E}} \nabla y_{\mathrm{E}}) \tag{54}$$

since $\operatorname{div} \mathbf{J}_{\mathrm{E}_q}$ =0, which states that the cation flux is simply diffusional w.r.t. the charge flux $\mathbf{J}_{\mathrm{E}_q}$. The (in general) non-linearly coupled balance equations decouple to a diffusion equation and a generalized ohmic law, i.e.

$$\begin{aligned} \frac{\partial n_{\mathrm{E}_C}}{\partial t} =& \operatorname{div} (\mathbf{D}_{\mathrm{E}} n_{\mathrm{E,tot}} \Gamma_{\mathrm{E}} \nabla y_{\mathrm{E}}) \,, && (55)\\ 0 =& \operatorname{div} (\mathbf{S}_{\mathrm{E}} n_{\mathrm{E,tot}} \Gamma_{\mathrm{E}} \nabla y_{\mathrm{E}} + n_{\mathrm{E,tot}} y_{\mathrm{E}} \mathbf{\Lambda}_{\mathrm{E}} \nabla \varphi_{\mathrm{E}}) \,, && (56) \end{aligned}$$

for which iterative numerical schemes can be designed. However, from a mathematical and thermodynamic point of view, the flux representations (25) are more convenient since they obey the positive semi-definiteness of the Onsager matrix $(M_{\alpha,\beta})_{\alpha,\beta}$. Hence we perform the up-scaling in Section 5 with the general representation (39)–(39) because of its favorable mathematical structure, and comment on representations in terms of the transport parameters (49) again later in section 6.2.2.

3.2 Solid Phase

The solid phase Ω_{S} is the union of the active phase $\Omega_{\mathtt{A}}$, where cations are stored in an intercalation electrode, and the conductive additive phase Ω_{C} which provides electronic contact among the (distinct) active phase particles.

The active particle phase $\Omega_{\mathtt{A}}$ is the host material for intercalated cations. For illustration, we examine only one porous electrode, applicable to both anode and cathode of a full battery. The active material is a mixture of host species $\mathtt{A}_M$ (e.g. Carbon in a graphite electrode), electrons $\mathtt{A}_e$, and intercalated cations $\mathtt{A}_C$, whereby $\mathcal{I}_{\mathtt{A}} = \{\mathtt{A}_M, \mathtt{A}_e, \mathtt{A}_C\}$ with corresponding molar densities $n_\alpha(\mathbf{x}, t)$. In the active particle phase $\Omega_{\mathtt{A}}$, we consider a lattice mixture model [9, 8, 24, 16, 18, 36, 37, 3, 12] with phase separation. The host species $\mathtt{A}_M$ form a lattice for the intercalated cations $\mathtt{A}_C$, and we denote with $n_{\mathtt{A},\mathrm{lat}} = \omega_{\mathtt{A},\mathrm{lat}} n_{\mathtt{A}_M}$ the molar density of lattice sites, where $\omega_{\mathtt{A},\mathrm{lat}}$ is the number of lattice sites per constituent $\mathtt{A}_M$, e.g. for Graphite with $\mathtt{A}_M = \mathrm{C}$ we have $\omega_{\mathtt{A},\mathrm{lat}} = \frac{1}{6}$ since 6 Carbon atoms provide one lattice site for a lithium atom, i.e. LiC_6. The lattice fraction of intercalated cations is then

$$y_{\mathtt{A}} = \frac{n_{\mathtt{A}_C}}{n_{\mathtt{A},\mathrm{lat}}}. \tag{57}$$

where $1 - y_{\mathtt{A}}$ corresponds to the lattice fraction of vacancies. We consider throughout this work an incompressible material (due to mixing/swelling), whereby $n_{\mathtt{A},\mathrm{lat}} = \text{const}$.[3]

The free energy density $\psi_{\mathtt{A}}$ consists of a reference contribution of the pure substances

$$\psi_{\mathtt{A}}^{\mathrm{ref}} = \sum_{\alpha \in \mathcal{I}_{\mathtt{A}}} n_\alpha g_\alpha \ , \tag{58}$$

a chemical part $\psi_{\mathtt{A}}^{\mathrm{chem}}$ and an interfacial part $\psi_{\mathtt{A}}^{\mathrm{int}}$, *i.e.* $\psi_{\mathtt{A}} = \psi_{\mathtt{A}}^{\mathrm{ref}} + \psi_{\mathtt{A}}^{\mathrm{chem}} + \psi_{\mathtt{A}}^{\mathrm{int}}$.

The chemical part of the free energy further splits into the contributions of mixing entropy $\psi_{\mathtt{A}}^{\mathrm{mix}}$ and mixing enthalpy $\psi_{\mathtt{A}}^{\mathrm{enth}}$, the latter actually triggering a phase separation (if its slope is negative enough), with

$$\psi_{\mathtt{A}}^{\mathrm{chem}} = \psi_{\mathtt{A}}^{\mathrm{mix}} + \psi_{\mathtt{A}}^{\mathrm{enth}} \tag{59}$$

$$\psi_{\mathtt{A}}^{\mathrm{mix}} = n_{\mathtt{A},\mathrm{lat}} y_{\mathtt{A}} \ln(y_{\mathtt{A}}) + n_{\mathtt{A},\mathrm{lat}} (1 - y_{\mathtt{A}}) \ln(1 - y_{\mathtt{A}_C}) \tag{60}$$

$$\psi_{\mathtt{A}}^{\mathrm{enth}} = \hat{\psi}_{\mathtt{A}}^{\mathrm{enth}}(y_{\mathtt{A}}) \ . \tag{61}$$

The classical enthalpy function $\hat{\psi}_{\mathtt{A}}^{\mathrm{enth}}(n_{\mathtt{A}_C})$ for Cahn-Hillard type mixtures is[37]

$$\hat{\psi}_{\mathtt{A}}^{\mathrm{enth}}(n_{\mathtt{A}_C}) = \eta_{\mathtt{A}} y_{\mathtt{A}} (1 - y_{\mathtt{A}}) \tag{62}$$

which yields for $\eta_{\mathtt{A}} > 2.5$ a double well potential for the chemical free energy $\psi_{\mathtt{A}}^{\mathrm{chem}}$ in terms of $y_{\mathtt{A}}$[4].

In this work, however, we want to consider also multi-well free energy functions, having more than two local minima for $y_{\mathtt{A}} \in (0, 1)$, *e.g.*

$$\psi_{\mathtt{A}}^{\mathrm{enth,n}} = -\frac{1}{n \cdot 2 \cdot \pi} \cos(n \cdot 2 \cdot \pi y_{\mathtt{A}}) + y_{\mathtt{A}}(1 - y_{\mathtt{A}}) \tag{63}$$

whereby $\psi_{\mathtt{A}}$ has $(n+1)$-local minima and thus $(n+1)$ stable phases.

[3] Note that this allows us to consider $y_{\mathtt{A}}$ equivalently as variable instead of $n_{\mathtt{A}_C}$

[4] Note that $\psi_{\mathtt{A}}^{\mathrm{chem}}$ are frequently approximated by polynomial expressions in $y_{\mathtt{A}}$.

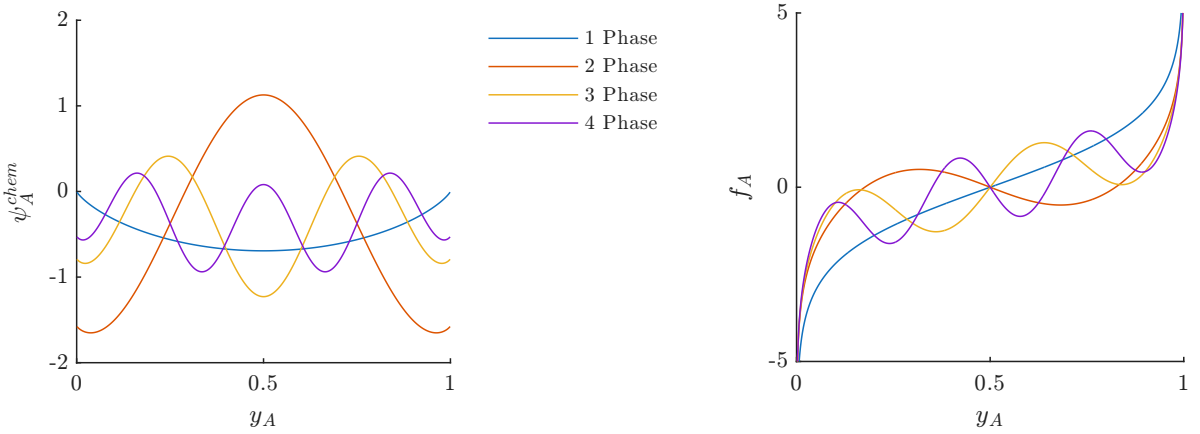

Figure 1: Chemical free energy energy density $\psi_{\mathtt{A}}^{\mathsf{chem}}$ (left) and the corresponding part $f_{\mathtt{A}}$ (right) of the chemical potential for stable multiple phases ($n = 0, 1, 2, 3$).

The interfacial free energy density is considered as

$$\psi_{\mathtt{A}}^{\mathsf{int}} = \frac{\gamma_{\mathtt{A}}}{2}|\nabla y_{\mathtt{A}_C}|^2 \tag{64}$$

which *drives* the phase separation due to the multi-well chemical free energy $\psi_{\mathtt{A}}^{\mathsf{chem}}$. The parameter $\gamma_{\mathtt{A}}$ encodes the thickness of the transition layer among the phases and we will discuss its scaling in section 5.

The overall free energy $\Psi_{\mathtt{A}}$ of the active phase is thus

$$\Psi_{\mathtt{A}} = \int_{\Omega_{\mathtt{A}}} (\psi_{\mathtt{A}}^{\mathsf{ref}} + \psi_{\mathtt{A}}^{\mathsf{mix}} + \psi_{\mathtt{A}}^{\mathsf{enth}} + \psi_{\mathtt{A}}^{\mathsf{int}}) dV \tag{65}$$

$$= \int_{\Omega_{\mathtt{A}}} \sum_{\alpha \in \mathcal{I}_{\mathtt{A}}} n_\alpha g_\alpha + n_{\mathtt{A},\mathsf{lat}} y_{\mathtt{A}} \ln(y_{\mathtt{A}}) + n_{\mathtt{A},\mathsf{lat}}(1-y_{\mathtt{A}})\ln(1-y_{\mathtt{A}_C}) + \hat{\psi}_{\mathtt{A}}^{\mathsf{enth}}(y_{\mathtt{A}}) + \frac{\gamma_{\mathtt{A}}}{2}|\nabla y_{\mathtt{A}_C}|^2) dV \,. \tag{66}$$

Similar to the electrolyte phase, we consider in the active phase also (strong) electro-neutrality, i.e.

$$q_{\mathtt{A}} = e_0(z_{\mathtt{A}_e} n_{\mathtt{A}_e} + z_{\mathtt{A}_M} n_{\mathtt{A}_M}) = 0 \,, \tag{67}$$

which determines $n_{\mathtt{A}_e} = z_{\mathtt{A}_M} n_{\mathtt{A}_M}$ as well as $p_{\mathtt{A}} = \text{const.}$, from the momentum balance, and reduces the variables for the active phase to $(y_{\mathtt{A}}, \varphi_{\mathtt{A}})$.

The relevant chemical potential functions thus read

$$\mu_{\mathtt{A}_e} = g_{\mathtt{A}_e} = \text{const.}(\text{ since } n_{\mathtt{A}_e} = \text{const.}) \tag{68}$$

$$\mu_{\mathtt{A}_C} = g_{\mathtt{A}_C} + k_{\mathtt{B}} T \, f_{\mathtt{A}}(y_{\mathtt{A}}) - \gamma_{\mathtt{A}} \operatorname{div} \nabla y_{\mathtt{A}} \tag{69}$$

with

$$f_{\mathtt{A}}(y_{\mathtt{A}}) := \ln\left(\frac{y_{\mathtt{A}}}{1+y_{\mathtt{A}}}\right) + h_{\mathtt{A}}(y_{\mathtt{A}}) \,, \qquad h_{\mathtt{A}} := \frac{\partial \hat{\psi}_{\mathtt{A}}^{\mathsf{enth}}}{\partial y_{\mathtt{A}}} \,. \tag{70}$$

For the two independent fluxes, i.e. the electron flux $\mathbf{J}_{\mathtt{A}_e}$ and the intercalated cation $\mathbf{J}_{\mathtt{A}_C}$ we consider (c.f. section 2.3)

$$\mathbf{J}_{\mathtt{A}_C} = -M_C^{\mathtt{A}} \frac{1}{k_{\mathtt{B}} T} \nabla \tilde{\mu}_{\mathtt{A}_C} \tag{71}$$

$$\mathbf{J}_{\mathtt{A}_e} = -M_e^{\mathtt{A}} \frac{1}{k_{\mathtt{B}} T} \nabla \tilde{\mu}_{\mathtt{A}_e} \tag{72}$$

with $\mathtt{A}_M$ as reference system. Cross-Diffusion could in general be considered in a similar way as in the electrolyte, but we restrict ourselves here to flux relations (71) and (72). Further, we assume throughout this work that $\frac{m_{\mathtt{A}_C}}{m_{\mathtt{A}_M}} \approx \frac{m_{\mathtt{A}_e}}{m_{\mathtt{A}_M}} \approx 0$ and

$$M_C^{\mathtt{A}} = n_{\mathtt{A},\mathsf{lat}} D_C^{\mathtt{A}} y_{\mathtt{A}_C} (1 - y_{\mathtt{A}_C}) \tag{73}$$

which accounts for reduced diffusivity due to crowding[34]. Hence we have

$$\frac{\partial n_{\mathtt{A}_C}}{\partial t} = -\operatorname{div} \mathbf{J}_{\mathtt{A}_C}, \qquad \mathbf{J}_{\mathtt{A}_C} = -n_{\mathtt{A},\mathsf{lat}} D_C^{\mathtt{A}} y_{\mathtt{A}_C} (1 - y_{\mathtt{A}_C}) \nabla \mu_{\mathtt{A}_C} \tag{74}$$

$$\mu_{\mathtt{A}_C} = f_{\mathtt{A}}(y_{\mathtt{A}}) - \nabla(\gamma_{\mathtt{A}} \operatorname{div} \nabla y_{\mathtt{A}}) \tag{75}$$

$$\frac{\partial n_{\mathtt{A}_e}}{\partial t} = -\operatorname{div} \mathbf{J}_{\mathtt{A}_e}, \qquad \mathbf{J}_{\mathtt{A}_e} = +M_e^{\mathtt{A}} \frac{e_0}{k_{\mathtt{B}} T} \nabla \varphi_{\mathtt{A}} \,. \tag{76}$$

Note that the charge flux $\mathbf{J}_{\mathtt{A}_q}$ is only governed by electrons, whereby

$$\mathbf{J}_{\mathtt{A}_q} = -e_0 \mathbf{J}_{\mathtt{A}_e} = -M_e^{\mathtt{A}} \frac{e_0^2}{k_{\mathtt{B}} T} \nabla \varphi_{\mathtt{A}} \,. \tag{77}$$

Since we assume strong electro-neutrality in the active phase we have as charge balance

$$0 = -\operatorname{div} \mathbf{J}_{\mathtt{A}_q} = \operatorname{div} \left(M_e^{\mathtt{A}} \frac{e_0^2}{k_{\mathtt{B}} T} \nabla \varphi_{\mathtt{A}} \right), \tag{78}$$

which determines the electric potential $\varphi_{\mathtt{A}}$ in the active phase.

The conductive phase is essentially a mixture of lattice species $\mathtt{C}_M$ and electrons $\mathtt{C}_e$. Since we do not consider any intercalation into the conductive additive phase $\Omega_{\mathtt{C}}$, we have actually a single balance equation for the electrons. Electron viz. charge flux is assumed to be continuous at active-particle - conductive additive interfaces, whereby it is convenient to introduce a single transport equation for the charge flux in the solid phase $\Omega_{\mathtt{S}} = \Omega_{\mathtt{A}} \cup \Omega_{\mathtt{C}}$

$$0 = -\operatorname{div} \mathbf{J}_{\mathtt{S}_q} \qquad \text{with} \quad \mathbf{J}_{\mathtt{S}_q} = -\sigma_{\mathtt{S}}(\mathbf{x}) \nabla \varphi_{\mathtt{S}} \tag{79}$$

where the electrostatic potential in the solid phase is denoted as $\varphi_{\mathtt{S}}(\mathbf{x}, t)$ with

$$\varphi_{\mathtt{S}} = \begin{cases} \varphi_{\mathtt{A}}, & \text{if } \mathbf{x} \in \Omega_{\mathtt{A}} \\ \varphi_{\mathtt{C}}, & \text{if } \mathbf{x} \in \Omega_{\mathtt{C}} \end{cases} \qquad \sigma_{\mathtt{S}}(\mathbf{x}) = \begin{cases} M_e^{\mathtt{A}} \frac{e_0^2}{k_{\mathtt{B}} T}, & \text{if } \mathbf{x} \in \Omega_{\mathtt{A}} \\ M_e^{\mathtt{C}} \frac{e_0^2}{k_{\mathtt{B}} T}, & \text{if } \mathbf{x} \in \Omega_{\mathtt{C}} \end{cases} . \tag{80}$$

3.3 Reaction Rates

At the surface $\Sigma_{\mathtt{AE}}$, the intercalation reaction

$$\mathtt{E}_C + \mathtt{A}_e \rightleftharpoons \mathtt{A}_C + \kappa_{\mathtt{E}} \cdot \mathtt{E}_S \,, \tag{81}$$

for instance $\mathrm{Li}^+ + \mathrm{e}^- \rightleftharpoons \mathrm{Li} + \kappa_{Li^+}\,\mathrm{S}$, takes place. This reaction is modeled using (surface) non-equilibrium thermodynamics [34]. As we have sketched in section 2.3, the (surface) reaction rate $\underset{s}{R}$ can be generally expressed as [35, 13, 20, 15, 19]

$$\underset{s}{R} = \underset{s}{L} \cdot f_{\mathtt{BV}}\left(\underset{s}{\lambda}\right), \qquad \text{with} \qquad f_{\mathtt{BV}}(z) := \left(\mathrm{e}^{\alpha\cdot z} - \mathrm{e}^{-(1-\alpha)\cdot z}\right), \tag{82}$$

where $\alpha \in [0,1]$ and (c.f. section 2.3)

$$\underset{s}{\lambda} = -\frac{1}{k_{\mathtt{B}}T}(\underset{s}{\mu}_{\mathtt{A}_C} + \kappa_{\mathtt{E}} \cdot \underset{s}{\mu}_{\mathtt{E}_S} - \mu_{\mathtt{E}_C} - \mu_{\mathtt{A}_e}) \tag{83}$$

denotes the surface affinity of the reaction (81). This affinity is *pulled back* through the double layer (c.f. section 2.4 to the corresponding *points* outside of the double layer at the interface $\Sigma_{\mathtt{AE}}$ in an asymptotic sense, yielding

$$\begin{aligned}\underset{s}{\lambda} &= -\frac{1}{k_{\mathtt{B}}T}(\tilde{\mu}_{\mathtt{A}_C}|_\Sigma - \tilde{\mu}_{\mathtt{E}_C}|_\Sigma - \tilde{\mu}_{\mathtt{A}_e}|_\Sigma) &(84)\\ &= -\frac{1}{k_{\mathtt{B}}T}\left(\mu_{\mathtt{A}_C}|_\Sigma + \kappa_{\mathtt{E}} \cdot \mu_{\mathtt{E}_S}(1-2y_{\mathtt{E}}|_\Sigma) - \mu_{\mathtt{E}_C}(y_{\mathtt{E}}|_\Sigma) - g_{\mathtt{A}_e} + e_0(\varphi_{\mathtt{A}}|_\Sigma - \varphi_{\mathtt{E}}|_\Sigma)\right). &(85)\end{aligned}$$

Quite similar to the flux representations, all of this affinity relations are useful in one or the other way. Note that $\mu_{\mathtt{A}_C}|_\Sigma$ refers to the evaluation of $\mu_{\mathtt{A}_C}$ at the interface Σ, meaning that the surface affinity (84) depends on the chemical potential at the interface Σ.

3.4 Summarizing the balance equations

The coupled electrode-electrolyte model with phase separation is thus

$$\begin{aligned}
\frac{\partial n_{\mathtt{E}_C}}{\partial t} &= -\operatorname{div}\mathbf{J}_{\mathtt{E}_C} \quad \text{with} \quad \mathbf{J}_{\mathtt{E}_C} = -\mathbf{M}^{\mathtt{E}}_{C,A}\frac{1}{k_{\mathtt{B}}T}\nabla\tilde{\mu}_{\mathtt{E}_A} - \mathbf{M}^{\mathtt{E}}_{C,C}\frac{1}{k_{\mathtt{B}}T}\nabla\tilde{\mu}_{\mathtt{E}_C} && \mathbf{x}\in\Omega_{\mathtt{E}} && (86)\\
\frac{\partial n_{\mathtt{E}_A}}{\partial t} &= -\operatorname{div}\mathbf{J}_{\mathtt{E}_A} \quad \text{with} \quad \mathbf{J}_{\mathtt{E}_A} = -\mathbf{M}^{\mathtt{E}}_{A,A}\frac{1}{k_{\mathtt{B}}T}\nabla\tilde{\mu}_{\mathtt{E}_A} - \mathbf{M}^{\mathtt{E}}_{A,C}\frac{1}{k_{\mathtt{B}}T}\nabla\tilde{\mu}_{\mathtt{E}_C} && \mathbf{x}\in\Omega_{\mathtt{E}} && (87)\\
0 &= -\operatorname{div}\mathbf{J}_{\mathtt{S}_q} \quad \text{with} \quad \mathbf{J}_{\mathtt{S}_q} = -\sigma_{\mathtt{S}}(\mathbf{x})\nabla\varphi_{\mathtt{S}} && \mathbf{x}\in\Omega_{\mathtt{S}} && (88)\\
\frac{\partial y_{\mathtt{A}_C}}{\partial t} &= -\operatorname{div}\mathbf{J}_{\mathtt{A}_C} \quad \text{with} \quad \mathbf{J}_{\mathtt{A}_C} = -\mathbf{M}^{\mathtt{A}}_{C}\frac{1}{k_{\mathtt{B}}T}\nabla\mu_{\mathtt{A}_C} && \mathbf{x}\in\Omega_{\mathtt{A}} && (89)
\end{aligned}$$

with

$$\mu_{\mathtt{A}_C} = g_{\mathtt{A}_C} + k_{\mathtt{B}}T\, f_{\mathtt{A}}(y_{\mathtt{A}}) - \gamma_{\mathtt{A}}\operatorname{div}\nabla y_{\mathtt{A}} \qquad \mathbf{x}\in\Omega_{\mathtt{A}} \tag{90}$$

and

$$\begin{aligned}
\frac{1}{2}(\tilde{\mu}_{\mathtt{E}_C} - \tilde{\mu}_{\mathtt{E}_A}) &= e_0\varphi_{\mathtt{E}} + \underbrace{\frac{1}{2}(g_{\mathtt{E}_C} - g_{\mathtt{A}_C})}_{=\text{const.}} &(91)\\
\frac{1}{2}(\tilde{\mu}_{\mathtt{E}_C} + \tilde{\mu}_{\mathtt{E}_A}) &= k_{\mathtt{B}}T\, f_{\mathtt{E}}(y_{\mathtt{E}}) + \underbrace{\frac{1}{2}(g_{\mathtt{E}_A} + g_{\mathtt{E}_C} - 2\kappa_{\mathtt{E}}g_{\mathtt{E}_S})}_{=\text{const.}}, &(92)
\end{aligned}$$

or alternatively for the electrolyte (eqs. (86) and (87))

$$\frac{\partial n_{\mathtt{E}_C}}{\partial t} = -\operatorname{div} \mathbf{J}_{\mathtt{E}_C} \qquad \text{with} \quad \mathbf{J}_{\mathtt{E}_C} = -\mathbf{D}_{\mathtt{E}} n_{\mathtt{E},\mathrm{tot}} \Gamma_{\mathtt{E}} \nabla y_{\mathtt{E}_C} + \frac{1}{z_C e_0} \mathbf{t}_{\mathtt{E}_C} \mathbf{J}_{\mathtt{E}_q} \qquad \mathbf{x} \in \Omega_{\mathtt{E}} \tag{93}$$

$$= -\mathbf{D}_{\mathtt{E}}^{y} \nabla y_{\mathtt{E}} - \mathbf{D}_{\mathtt{E}}^{\varphi} \nabla \varphi_{\mathtt{E}} \qquad \mathbf{x} \in \Omega_{\mathtt{E}} \tag{94}$$

$$0 = -\operatorname{div} \mathbf{J}_{\mathtt{E}_q} \qquad \text{with} \quad \mathbf{J}_{\mathtt{E}_q} = -\mathbf{S}_{\mathtt{E}} n_{\mathtt{E},\mathrm{tot}} \Gamma_{\mathtt{E}} \nabla y_{\mathtt{E}_C} - n_{\mathtt{E},\mathrm{tot}} y_{\mathtt{E}} \mathbf{\Lambda}_{\mathtt{E}} \nabla \varphi_{\mathtt{E}} \qquad \mathbf{x} \in \Omega_{\mathtt{E}} \,. \tag{95}$$

Eq. (89) is the balance of intercalated lithium within the active phase, (88) the charge balance in the solid phase and $(87)_2$ the electron flux, (86) and (87) the balance of cations and anions in the electrolyte phase and (95) the charge balance in the electrolyte, where $(95)_2$ is the flux of the charge $q_{\mathtt{E}}$. Note that $\sigma_{\mathtt{S}}(\mathbf{x})$ incorporates the fact that the conductivity is far larger in the conductive additive phase $\Omega_{\mathtt{C}}$ then in the active particle phase $\Omega_{\mathtt{A}}$.

The boundary conditions at the interface $\Sigma_{\mathtt{AE}} = \Omega_{\mathtt{A}} \cap \Omega_{\mathtt{E}}$, where the intercalation reaction $\mathrm{Li}^+ + \mathrm{e}^- \rightleftharpoons \mathrm{Li}$ occurs ($\mathbf{n}$ is pointing from $\Omega_{\mathtt{A}}$ into $\Omega_{\mathtt{E}}$, *i.e.* is the normal vector of $\partial\Omega_{\mathtt{A}}$),

$$\mathbf{J}_{\mathtt{A}_C} \cdot \mathbf{n} = \mathbf{J}_{\mathtt{E}_C} \cdot \mathbf{n} = -\underset{s}{L} \cdot g\big(\underset{s}{\lambda}\big) \tag{96}$$

$$\mathbf{J}_{\mathtt{S}_q} \cdot \mathbf{n} = \mathbf{J}_{\mathtt{E}_q} \cdot \mathbf{n} = -e_0 \underset{s}{L} \cdot g\big(\underset{s}{\lambda}\big) \tag{97}$$

$$\underset{s}{\lambda} = -\frac{1}{k_{\mathtt{B}} T} (\tilde{\mu}_{\mathtt{A}_C}|_{\Sigma} - \tilde{\mu}_{\mathtt{E}_C}|_{\Sigma} - \tilde{\mu}_{\mathtt{A}_e}|_{\Sigma}) \tag{98}$$

$$= -\big(\Delta g_{\mathtt{AE}} + f_{\mathtt{A}}(y_{\mathtt{A}}|_{\Sigma}) - \frac{\gamma_{\mathtt{A}}}{k_{\mathtt{B}} T} (\operatorname{div} \nabla y_{\mathtt{A}})|_{\Sigma} - f_{\mathtt{E}}(y_{\mathtt{E}}|_{\Sigma}) + \frac{e_0}{k_{\mathtt{B}} T} (\varphi_{\mathtt{A}}|_{\Sigma} - \varphi_{\mathtt{E}}|_{\Sigma})\big) \tag{99}$$

with

$$\Delta g_{\mathtt{AE}} = k_{\mathtt{B}} T \left(g_{\mathtt{A}_C} - g_{\mathtt{E}_C} + \kappa_{\mathtt{E}} g_{\mathtt{E}_S} - g_{\mathtt{A}_e} \right), \tag{100}$$

where by convention $\mathbf{n}$ is pointing from $\Omega_{\mathtt{A}}$ into $\Omega_{\mathtt{E}}$. The anions from the electrolyte are non-reactive, wherby we have

$$\mathbf{J}_{\mathtt{A}_C} \cdot \mathbf{n}|_{\Sigma} = 0 \,. \tag{101}$$

Note this formulation of the boundary conditions neglects double layer *charging*, i.e. currents arising from temporal variations of the boundary layer charge [43, 34, 35], which are rather small compared to the intercalation current [34]. At the interface $\Sigma_{\mathtt{CE}} = \Omega_{\mathtt{C}} \cap \Omega_{\mathtt{E}}$ we have homogenous Neumann boundary conditions, *i.e.* no insertion from the electrolyte into the conductive additive phase,

$$\mathbf{J}_{\mathtt{A}_C} \cdot \mathbf{n} = \mathbf{J}_{\mathtt{S}_q} \cdot \mathbf{n} = \mathbf{J}_{\mathtt{E}_C} \cdot \mathbf{n} = \mathbf{J}_{\mathtt{E}_q} \cdot \mathbf{n} = 0 \qquad \text{on } \Sigma_{\mathtt{CE}} \,. \tag{102}$$

Further we have a *global* boundary condition for the electric current[5] density i entering (charge, $i < 0$) or leaving (discharge, $i > 0$) the porous electrode via the current collector, *i.e.*

$$\mathbf{J}_{\mathtt{S}_q} \cdot \mathbf{n} = -i \qquad \text{on } \Sigma_{\mathtt{CC}} \subset \partial\Omega_{\mathtt{S}} \,. \tag{103}$$

[5]Note that IUPAC definition, and also our definition of current $i = -e_0 J_{\mathtt{A}_e}$, implies for $i > 0$ a negative electron flux. Hence, if $i < 0$, electrons enter the electrode while for $i > 0$ electrons leave the electrode. That is reflected in the sign of eq. (103).

4 Half cell setup and boundary conditions

4.1 Cell voltage and boundary conditions reflecting a counter electrode

We consider in this work an electrochemical cell composed of a (porous) working electrode, a separator, and a metallic counter electrode, e.g. a metallic lithium foil, where we do not spatially resolve the separator and the counter electrode. In contrast, we assume that the counter electrode is large compared to the porous electrode whereby the metallic dissolution reaction

$$\mathrm{M}_C + \kappa_{\mathrm{E}_C}\mathrm{E}_S \rightleftharpoons \mathrm{E}_C \tag{104}$$

is assumed to be in equilibrium. Further, the electronic conductivity of the counter electrode is assumed to be very high, yielding a constant voltage value $\varphi_{\mathtt{M}}$. Since the whole mathematical problem is determined up to a constant shift in φ, we may set $\varphi^{\mathtt{M}} = 0$ which yields essentially a constraint at the boundary $\Sigma_{\mathtt{E}}$,

$$\frac{e_0}{k_{\mathtt{B}}T}(\varphi_{\mathtt{E}}|_{\Sigma_{\mathtt{EE}}}) = -\Delta g^{\mathsf{di}}_{\mathtt{EM}} - f_{\mathtt{E}}(y_{\mathtt{E}}|_{\Sigma_{\mathtt{EE}}}) \,, \tag{105}$$

relating the bulk concentration $y_{\mathtt{E}}|_{\Sigma_{\mathtt{EE}}}$ and the bulk electrolyte potential $\varphi_{\mathtt{E}}|_{\Sigma_{\mathtt{EE}}}$. We assume further throughout this work, that the electrolyte concentration does not change in the bulk, *i.e.* $y_{\mathtt{E}}|_{\Sigma_{\mathtt{E}}} = y^{\mathsf{init}}_{\mathtt{E}}$, whereby we obtain the Dirichlet conditions

$$\varphi_{\mathtt{E}}|_{\Sigma_{\mathtt{EE}}} = -\frac{k_{\mathtt{B}}T}{e_0}(\Delta g^{\mathsf{di}}_{\mathtt{EM}} - f_{\mathtt{E}}(y^{\mathsf{init}}_{\mathtt{E}})) \tag{106}$$

$$y_{\mathtt{E}}|_{\Sigma_{\mathtt{E}}} = y^{\mathsf{init}}_{\mathtt{E}} \,. \tag{107}$$

The **cell voltage** is related to the (electrochemical) potential of the electrons [28, 33, 34, 35, 37] in the different phases which yields

$$E = -\frac{1}{e_0}(\tilde{\mu}_{\mathtt{A}_e}|_{\Sigma_{\mathtt{CC}}} - \tilde{\mu}_{\mathtt{M}_e}) \tag{108}$$

$$= \varphi^{\mathtt{S}}|_{\Sigma_{\mathtt{CC}}} - e_0(g_{\mathtt{A}_e} - g_{\mathtt{M}_e}) \,. \tag{109}$$

4.2 Initial conditions and convenient variable transformations

We consider the initial conditions

$$y_{\mathtt{A}}(\mathbf{x}, t=0) = y^{\mathsf{init}}_{\mathtt{A}} \,, \qquad \varphi_{\mathtt{A}}(\mathbf{x}, t=0) = \varphi^{\mathsf{init}}_{\mathtt{A}} \qquad \mathbf{x} \in \Omega_{\mathtt{A}} \tag{110}$$

$$y_{\mathtt{E}}(\mathbf{x}, t=0) = y^{\mathsf{init}}_{\mathtt{E}} \,, \qquad \varphi_{\mathtt{E}}(\mathbf{x}, t=0) = \varphi^{\mathsf{init}}_{\mathtt{E}} \qquad \mathbf{x} \in \Omega_{\mathtt{E}} \,. \tag{111}$$

where $\varphi^{\mathsf{init}}_{\mathtt{A}}$ and $\varphi^{\mathsf{init}}_{\mathtt{E}}$ are *a priori* unknown.

However, without any current flowing in the initial state, we can deduce from the (necessary) reaction equilibrium $\underset{s}{\lambda}(t=0) \overset{!}{=} 0$ (c.f. equation (98)) necessary conditions for the initial values of φ, i.e.

$$\frac{e_0}{k_{\mathtt{B}}T}(\varphi^{\mathsf{init}}_{\mathtt{S}} - \varphi^{\mathsf{init}}_{\mathtt{E}}) \overset{!}{=} -\Delta g_{\mathtt{AE}} + f_{\mathtt{E}}(y^{\mathsf{init}}_{\mathtt{E}}) - f_{\mathtt{A}}(y^{\mathsf{init}}_{\mathtt{A}}) \,. \tag{112}$$

These are sometimes also called *compatibility conditions* of the initial values.

Together with eq. (106) the initial values for φ are thus determined as

$$\frac{e_0}{k_{\mathtt{B}}T}\varphi_{\mathtt{E}}^{\mathsf{init}} = -(\Delta g_{\mathtt{EM}}^{\mathsf{di}} + f_{\mathtt{E}}(y_{\mathtt{E}_C}^{\mathsf{init}})) \tag{113}$$

$$\frac{e_0}{k_{\mathtt{B}}T}\varphi_{\mathtt{S}}^{\mathsf{init}} = -\big(\Delta g_{\mathtt{AE}} + \Delta g_{\mathtt{EM}}^{\mathsf{di}} + f_{\mathtt{A}}(y_{\mathtt{A}}^{\mathsf{init}})\big) \tag{114}$$

We introduce thus the variable transformations ($j = \mathtt{A}, \mathtt{E}$, $\alpha = \mathtt{E}_C, \mathtt{E}_A$)

$$\hat{\varphi}_j := \frac{e_0}{k_{\mathtt{B}}T}(\varphi_j - \varphi_j^{\mathsf{init}}) \tag{115}$$

$$\hat{\mu}_\alpha := \frac{1}{k_{\mathtt{B}}T}(\tilde{\mu}_\alpha - \tilde{\mu}_\alpha^{\mathsf{init}}) \tag{116}$$

$$\hat{f}_j(y_j) := f_j(y_j) - f_j(y_j^{\mathsf{init}}) \tag{117}$$

which yields

$$\frac{1}{2}(\hat{\mu}_{\mathtt{E}_C} - \hat{\mu}_{\mathtt{E}_A}) = \hat{\varphi}_{\mathtt{E}} \tag{118}$$

$$\frac{1}{2}(\hat{\mu}_{\mathtt{E}_C} + \hat{\mu}_{\mathtt{E}_A}) = \hat{f}_{\mathtt{E}}(y_{\mathtt{E}}) \tag{119}$$

as well as the following convenient expression for the intercalation reaction affinity,

$$\underset{s}{\lambda} = -\frac{1}{k_{\mathtt{B}}T}(\hat{\mu}_{\mathtt{A}_C}|_\Sigma - \hat{\mu}_{\mathtt{E}_C}|_\Sigma + e_0\hat{\varphi}_{\mathtt{S}}|_\Sigma) \tag{120}$$

$$= -\big(\hat{f}_{\mathtt{A}}(y_{\mathtt{A}}|_\Sigma) + \frac{\gamma_{\mathtt{A}}}{k_{\mathtt{B}}T}(\operatorname{div}\nabla y_{\mathtt{A}})|_\Sigma - \hat{f}_{\mathtt{E}}(y_{\mathtt{E}}|_\Sigma) + \hat{\varphi}_{\mathtt{A}}|_\Sigma - \hat{\varphi}_{\mathtt{E}}|_\Sigma\big)\ . \tag{121}$$

Note that for the re-scaled potential values $\hat{\varphi}$ and functions $\hat{f}$ we have

$$\hat{\varphi}_{\mathtt{A}}^{\mathsf{init}} = \hat{\varphi}_{\mathtt{E}}^{\mathsf{init}} = 0 \quad \text{and} \quad \hat{f}_{\mathtt{A}}(y_{\mathtt{A}}^{\mathsf{init}}) = f_{\mathtt{E}}(y_{\mathtt{E}}^{\mathsf{init}}) = 0\ . \tag{122}$$

4.3 Scalings and Non-Dimensionalization

To introduce proper scalings and non-dimensionalizations, some definitions of important (global) quantities are required. For a lithium ion battery, the following quantities are of most importance:

1 the cell voltage $E = \varphi^{\mathsf{S}}|_{\Sigma_{\mathtt{CC}}} - e_0(g_{\mathtt{A}_e} - g_{\mathtt{M}_e})$ [V],

2 the total (electrode) capacity $Q^0 = \int_{\Omega^A} q_{\mathtt{A}}, dV$, [Ah] with $q_{\mathtt{A}} = e_0 n_{\mathtt{A},\mathsf{lat}}$,

3 the present (electrode) capacity $Q(t) = \int_{\Omega^A} q_{\mathtt{A}} y_{\mathtt{A}}(\mathbf{x}, t)dV$, [Ah],

4 the (electrode) status of charge $\bar{\bar{y}}_{\mathtt{A}}(t) := \frac{Q(t)}{Q^0} = \frac{1}{|\Omega_{\mathtt{A}}|}\int_{\Omega_{\mathtt{A}}} y_{\mathtt{A}}(\mathbf{x}, t)dV$,

5 the 1-C current density $i_C = \frac{Q^0}{|\Sigma_{\mathtt{C}}|\cdot 1[\mathsf{h}]} = \frac{\mathscr{L} q_{\mathtt{A}}\psi_{\mathtt{A}}}{1[\mathsf{h}]}$, [Am^{-2}], where $\Sigma_{\mathtt{C}}$ is the area of the current collector and $\psi_{\mathtt{A}} = \frac{|\Omega_{\mathtt{A}}|}{|\Omega|}$ the volume fraction of the active phase $\Omega_{\mathtt{A}}$. This introduces the for the current density i the scaling $i = C_h \cdot i_C$, where $C_h \in \mathbb{R}$ is the C-Rate,

6 and the global current $I = i \cdot |\Sigma_{\mathtt{C}}|$.

Note that

$$Q(t)-Q^0 = \int_0^t I\,dt\,. \tag{123}$$

For a constant discharge current we obtain thus

$$\bar{y}_{\mathtt{A}}(t) - \bar{y}_{\mathtt{A}}(t=0) = \frac{C_h}{1\,[\mathsf{h}]}\cdot t\,, \tag{124}$$

which introduces the time-scaling $\tau = \frac{C_h}{1[\mathsf{h}]}\cdot t$.

4.3.1 Scalings

$$n_{\mathtt{E},\mathsf{tot}} = n_{\mathtt{E}_S}\cdot\frac{1}{1+2(\kappa_{\mathtt{E}}-1)y_{\mathtt{E}}} = n_{\mathtt{E},\mathsf{tot}}(y_{\mathtt{E}}), \tag{125}$$

$$n_{\mathtt{E}_C} = n_{\mathtt{E}_S}\frac{y_{\mathtt{E}}}{1+2(\kappa_{\mathtt{E}}-1)y_{\mathtt{E}}} = n_{\mathtt{E}_C}(y_{\mathtt{E}}). \tag{126}$$

In order to non-dimensionalize the equation system (86) – (95) together with its boundary conditions (96),(97),(98),(102),(103), we introduce the following scalings:

4.3.2 Dimensionless balance eqution s

Hence we obtain the dimensionless balance equations

$$C_h\frac{\partial y_{\mathtt{A}_C}}{\partial\tau} = -\operatorname{div}_\xi\varepsilon^2\hat{\mathbf{J}}_{\mathtt{A}_C} \quad \text{with} \quad \hat{\mathbf{J}}_{\mathtt{A}_C} = -\hat{M}_{\mathtt{A}}\nabla_\xi\hat{\mu}_{\mathtt{A}} \qquad \mathbf{x}\in\Omega_{\mathtt{A}}\,, \tag{127}$$

$$0 = -\operatorname{div}_\xi\hat{\mathbf{J}}_{\mathtt{S}_q} \quad \text{with} \quad \hat{\mathbf{J}}_{\mathtt{S}_q} = -\tilde{\sigma}_{\mathtt{S}}(\mathbf{x})\nabla_\xi\tilde{\varphi}_{\mathtt{S}} \qquad \mathbf{x}\in\Omega_{\mathtt{S}}\,, \tag{128}$$

$$C_h c_{\mathtt{E}}\frac{\partial y_{\mathtt{E}}}{\partial\tau} = -\operatorname{div}\hat{\mathbf{J}}_{\mathtt{E}_C} \quad \text{with} \quad \hat{\mathbf{J}}_{\mathtt{E}_C} = -\hat{\mathbf{M}}_{C,A}\nabla_\xi\hat{\mu}_{\mathtt{E}_A} - \hat{\mathbf{M}}_{C,C}\nabla_\xi\hat{\mu}_{\mathtt{E}_C} \qquad \mathbf{x}\in\Omega_{\mathtt{E}} \tag{129}$$

$$c_{\mathtt{E}}\frac{\partial y_{\mathtt{E}}}{\partial\tau} = -\operatorname{div}\hat{\mathbf{J}}_{\mathtt{E}_A} \quad \text{with} \quad \hat{\mathbf{J}}_{\mathtt{E}_A} = -\hat{\mathbf{M}}_{A,A}\nabla_\xi\hat{\mu}_{\mathtt{E}_A} - \hat{\mathbf{M}}_{A,C}\nabla_\xi\hat{\mu}_{\mathtt{E}_C} \qquad \mathbf{x}\in\Omega_{\mathtt{E}} \tag{130}$$

with

$$\hat{\mu}_{\mathtt{A}_C} = \hat{f}_{\mathtt{A}}(y_{\mathtt{A}}) - \tilde{\gamma}_{\mathtt{A}}\varepsilon^2\operatorname{div}\nabla_\xi y_{\mathtt{A}} \qquad \mathbf{x}\in\Omega_{\mathtt{A}} \tag{131}$$

and

$$\frac{1}{2}(\hat{\mu}_{\mathtt{E}_C} - \hat{\mu}_{\mathtt{E}_A}) = \tilde{\varphi}_{\mathtt{E}} \tag{132}$$

$$\frac{1}{2}(\hat{\mu}_{\mathtt{E}_C} + \hat{\mu}_{\mathtt{E}_A}) = \hat{f}_{\mathtt{E}}(y_{\mathtt{E}})\,. \tag{133}$$

Note that we can substitute (129) and (130) by the equations

$$C_h\hat{c}_{\mathtt{E}}(y_{\mathtt{E}})\frac{\partial y_{\mathtt{E}}}{\partial\tau} = -\operatorname{div}\hat{\mathbf{J}}_{\mathtt{E}_C} \quad \text{with} \quad \hat{\mathbf{J}}_{\mathtt{E}_C} = -\hat{D}^y_{\mathtt{E}}(y_{\mathtt{E}})\nabla_\xi y_{\mathtt{E}} - \hat{D}^\varphi_{\mathtt{E}}(y_{\mathtt{E}})\nabla_\xi\hat{\varphi}_{\mathtt{E}} \qquad \mathbf{x}\in\Omega_{\mathtt{E}} \tag{134}$$

$$0 = -\operatorname{div}\hat{\mathbf{J}}_{\mathtt{E}_q} \quad \text{with} \quad \hat{\mathbf{J}}_{\mathtt{E}_q} = -\hat{S}_{\mathtt{E}}(y_{\mathtt{E}})\nabla_\xi y_{\mathtt{E}} - \hat{\sigma}_{\mathtt{E}}(y_{\mathtt{E}})\nabla_\xi\hat{\varphi}_{\mathtt{E}} \qquad \mathbf{x}\in\Omega_{\mathtt{E}}. \tag{135}$$

Table 1: Definition of nondimensional variables, scaling and material functions

Variables	
Time scaling	$t = \dfrac{1\,[\mathsf{h}]}{C_h}\,\tau, \quad \tau \in [0,1]$
Spatial scaling	$x = \xi\,\mathscr{L}, \quad \xi \in [0,1]$
Electrical current scaling	$i = C_h\, i_C\, \hat{i}(\tau), \quad i_C = \dfrac{Q^0}{1\,[\mathsf{h}]} = \dfrac{\mathscr{L}\psi_{\mathtt{A}} q_{\mathtt{A}}}{1\,[\mathsf{h}]}$
Micro-Macro aspect ratio	$\varepsilon = \dfrac{\ell}{\mathscr{L}}$
Chemical potentials	$\hat{\mu}_\alpha = \dfrac{1}{k_{\mathsf{B}}T}(\tilde{\mu}_\alpha - \tilde{\mu}_\alpha^{\mathsf{init}}), \quad \alpha = \mathtt{E}_C, \mathtt{E}_A$
Electric potentials	$\hat{\varphi}_j = \dfrac{e_0}{k_{\mathsf{B}}T}(\varphi_j - \varphi_j^{\mathsf{init}}), \quad j = \mathtt{A}, \mathtt{E}$
Active material chemical potential	$\hat{\mu}_{\mathtt{A}} = \dfrac{1}{k_{\mathsf{B}}T}\mu_{\mathtt{A}}$
Free energy shift	$\hat{f}_j(y_j) = f_j(y_j) - f_j(y_j^{\mathsf{init}}), \quad j = \mathtt{A}, \mathtt{E}$
Electrolyte	
Cation concentration	$n_{\mathtt{E}_C} = \hat{n}_{\mathtt{E},\mathsf{tot}}\, n_{\mathtt{E},\mathsf{ref}}\, y_{\mathtt{E}}, \quad y_{\mathtt{E}} \in [0,1]$
Total concentration	$\hat{n}_{\mathtt{E},\mathsf{tot}} = \dfrac{n_{\mathtt{E},\mathsf{tot}}}{n_{\mathtt{E},\mathsf{ref}}} = \dfrac{1}{1 + 2(\kappa_{\mathtt{E}} - 1)y_{\mathtt{E}}}$
Capacity factor	$\hat{c}_{\mathtt{E}} = \dfrac{\partial n_{\mathtt{E}_C}(y_{\mathtt{E}})}{n_{\mathtt{E},\mathsf{ref}}\,\partial y_{\mathtt{E}}} = \dfrac{1}{(1 + 2(\kappa_{\mathtt{E}} - 1)y_{\mathtt{E}})^2}$
Stoichiometric ratio	$\eta_q = \dfrac{n_{\mathtt{A},\mathsf{lat}}}{n_{\mathtt{E},\mathsf{ref}}}$
Conductivity	$\hat{\sigma}_{\mathtt{E}} = \hat{\Lambda}_{\mathtt{E}}\, \hat{n}_{\mathtt{E},\mathsf{tot}}(y_{\mathtt{E}})\, y_{\mathtt{E}}, \quad \text{with} \quad \hat{\Lambda}_{\mathtt{E}} = \eta_q \dfrac{1\,[\mathsf{h}]}{\ell^2} \dfrac{k_{\mathsf{B}}T}{e_0^2} \Lambda_{\mathtt{E}}$
Diffusivity	$\hat{D}_{\mathtt{E}} = \hat{D}_{\mathtt{E}}^0\, \hat{n}_{\mathtt{E},\mathsf{tot}}(y_{\mathtt{E}})\, \Gamma_{\mathtt{E}}(y_{\mathtt{E}}), \quad \text{with} \quad \hat{D}_{\mathtt{E}}^0 = \eta_q \dfrac{1\,[\mathsf{h}]}{\mathscr{L}^2} D_{\mathtt{E}}$
Electrolyte free energy	$f_{\mathtt{E}} = \mathsf{ln}\,(y)_{\mathtt{E}} - \kappa_{\mathtt{E}} \mathsf{ln}\,(1 - 2y_{\mathtt{E}})$
Thermodynamic factor	$\Gamma_{\mathtt{E}} = 1 + \kappa_{\mathtt{E}} \dfrac{2y_{\mathtt{E}}}{1 - 2y_{\mathtt{E}}} = y_{\mathtt{E}} \dfrac{\partial f_{\mathtt{E}}}{\partial y_{\mathtt{E}}}$
Electro-diffusion coupling coefficient	$\hat{S}_{\mathtt{E}} = \hat{S}_{\mathtt{E}}^0\, n_{\mathtt{E},\mathsf{tot}}(y_{\mathtt{E}})\, \Gamma_{\mathtt{E}}(y_{\mathtt{E}}), \quad \text{with} \quad \hat{S}_{\mathtt{E}}^0 = \eta_q \dfrac{1}{e_0} \dfrac{1\,[\mathsf{h}]}{\mathscr{L}^2} S_{\mathtt{E}}$
Conversion relations	$\hat{D}_{\mathtt{E}}^y = \hat{D}_{\mathtt{E}} + t_{\mathtt{E}_C} \hat{S}_{\mathtt{E}}, \quad \text{and} \quad \hat{D}_{\mathtt{E}}^\varphi = t_{\mathtt{E}_C} \hat{\sigma}_{\mathtt{E}}$
Solid and Active Phase	
Intercalated cation density	$n_{\mathtt{A}_C} = n_{\mathtt{A},\mathsf{lat}} y_{\mathtt{A}}, \quad \text{with} \quad y_{\mathtt{A}} \in [0,1]$
Interfacial width parameter	$\hat{\gamma}_{\mathtt{A}} = \dfrac{\gamma_{\mathtt{A}}}{\ell^2 k_{\mathsf{B}}T}$
Mobility	$\hat{M}_{\mathtt{A}} = \hat{D}_{\mathtt{A}}^0\, y_{\mathtt{A}}(1 - y_{\mathtt{A}}), \quad \text{with} \quad \hat{D}_{\mathtt{A}}^0 = \dfrac{1\,[\mathsf{h}]}{\ell^2} D_C^{\mathtt{A}}$
Solid conductivity	$\hat{\sigma}_{\mathtt{S}} = \dfrac{1\,[\mathsf{h}]}{\ell^{\alpha_S} \mathscr{L}^{2-\alpha_S}} \dfrac{k_{\mathsf{B}}T\,/e_0^2}{n_{\mathtt{A},\mathsf{lat}}^j}\, \sigma_{\mathtt{S}}$
Intercalation reaction rate	$\hat{L} = \dfrac{1}{n_{\mathtt{A},\mathsf{lat}}} \big(1\,[\mathsf{h}]\,\big) \dfrac{1}{\ell}\, \dfrac{L}{s}$

Further, we have the boundary conditions

$$\varepsilon^2 \hat{\mathbf{J}}_{\mathtt{A}_C} \cdot \mathbf{n} = -\varepsilon \hat{L} \cdot g\big(\hat{\lambda}\big) \qquad \text{on } \Sigma_{\mathtt{AE}}\,, \tag{136}$$

$$\hat{\mathbf{J}}_{\mathtt{S}_q} \cdot \mathbf{n} = -\varepsilon \hat{L} \cdot g\big(\hat{\lambda}\big) \qquad \text{on } \Sigma_{\mathtt{AE}}\,, \tag{137}$$

$$\hat{\mathbf{J}}_{\mathtt{E}_C} \cdot \mathbf{n} = -\varepsilon \hat{L} g\big(\hat{\lambda}\big) \qquad \text{on } \Sigma_{\mathtt{AE}}\,, \tag{138}$$

$$\hat{\mathbf{J}}_{\mathtt{E}_A} \cdot \mathbf{n} = 0 \qquad \text{on } \Sigma_{\mathtt{AE}}\,, \tag{139}$$

$$\hat{\mathbf{J}}_{\mathtt{E}_q} \cdot \mathbf{n} = -\varepsilon \hat{L} \cdot g\big(\hat{\lambda}\big) \qquad \text{on } \Sigma_{\mathtt{AE}}\,, \tag{140}$$

$$\lambda = -(\hat{\mu}_{\mathtt{A}_C} - \hat{\mu}_{\mathtt{E}_C} + \hat{\varphi}_{\mathtt{S}}) \qquad \text{on } \Sigma_{\mathtt{AE}}\,, \tag{141}$$

$$= -\big(\hat{f}_{\mathtt{A}}(y_{\mathtt{A}}) - \hat{\gamma}_{\mathtt{A}}(\operatorname{div}_\xi \nabla_\xi y_{\mathtt{A}}) - \hat{f}_{\mathtt{E}}(y_{\mathtt{E}}) + \hat{\varphi}_{\mathtt{S}} - \hat{\varphi}_{\mathtt{E}}\big) \qquad \text{on } \Sigma_{\mathtt{AE}} \tag{142}$$

$$g(\lambda) = \mathsf{e}^{\alpha\lambda} - \mathsf{e}^{-(1-\alpha)\lambda} \tag{143}$$

and

$$\hat{\mathbf{J}}_{\mathtt{S}_q} \cdot \mathbf{n} = -\psi_{\mathtt{A}}^{\mathsf{Cat}} C_h \hat{i}(\tau) \qquad \text{on } \Sigma_{\mathtt{CC}}\,. \tag{144}$$

The initial values read

$$y_{\mathtt{A}} = y_{\mathtt{A}}^0 \qquad \hat{\varphi}_{\mathtt{S}} = 0 \tag{145}$$

$$y_{\mathtt{E}} = y_{\mathtt{A}}^0 \qquad \hat{\varphi}_{\mathtt{E}} = 0\,. \tag{146}$$

In order to derive a homogenized equation framework for the porous intercalation electrode, we properly set up the ε-problem and formulate a two-scale model in terms of multi-scale asymptotic expansions in the following.

5 The ε-problem and the two-scale model

5.1 Geometric setup

We start by considering the unit cube $Z \subset \mathbb{R}^3$ given by

$$\mathcal{Z} = (0,1)^3.$$

Within this cube, we define a ball $\mathcal{Z}_{\mathtt{A}} \subset \mathcal{Z}$ of radius $r_{\mathtt{A}} < \frac{1}{2}$ (Active phase), connecting rods $\mathcal{Z}_{\mathtt{C}} \subset \mathcal{Z}$ of radius $r_{\mathtt{C}}$ (Conductive additives), which form together Solid phase $\mathcal{Z}_{\mathtt{S}} = \mathcal{Z}_{\mathtt{A}} \cup \mathcal{Z}_{\mathtt{C}}$. Its complement $\mathcal{Z}_{\mathtt{E}} = \mathcal{Z} \setminus \mathcal{Z}_{\mathtt{S}}$ is denoted as Electrolyte phase. We define $\mathbf{n}_j$ as the outer normal vectors of $\mathcal{Z}_j$, $j = \mathtt{A}, \mathtt{C}, \mathtt{S}, \mathtt{E}$.

Next, we extend this geometric configuration periodically to the entire space $\mathbb{R}^3$. Specifically, we replicate $\mathcal{Z}$ periodically and scale the resulting structure by a factor of $\varepsilon > 0$. The small parameter $\varepsilon = \frac{\ell}{\mathscr{L}}$ is the size ratio of the active phase particle $\mathcal{Z}$ (*i.e.* the box width ℓ) with the macroscopic length scale $\mathscr{L}$ of the porous electrode (or equivalently, $\varepsilon \propto (N_{\mathtt{A}})^{\frac{1}{3}}$ where $N_{\mathtt{A}}$ is the number of active phase particles). The resulting sets are denoted by $\mathcal{Z}_j^\varepsilon, j = \mathtt{A}, \mathtt{C}, \mathtt{S}, \mathtt{E}$ and given by:

$$\mathcal{Z}_j^\varepsilon = \varepsilon \mathcal{Z}_j + \varepsilon \mathbb{Z}^3\,.$$

We now consider the reference domain $\Omega = (0,1)^3 \subset \mathbb{R}^3$, and define its intersections with $\mathcal{Z}_j^\varepsilon$ follows:

$$\Omega_j^\varepsilon = \Omega \cap \mathcal{Z}_j^\varepsilon, \quad j = \mathtt{A}, \mathtt{C}, \mathtt{S}, \mathtt{E}$$

Next, we define the following boundaries for the given domains:

- $\partial\Omega$: The boundary of the unit cube $\Omega = (0,1)^3$
- $\Sigma_{\mathtt{C}} = \{0\} \times (0,1)^2 \subset \partial\Omega$: The *left boundary* of the (porous) electrode
- $\Sigma_{\mathtt{E}} = \{1\} \times (0,1)^2 \subset \partial\Omega$: The *right boundary* of the (porous) electrode
- $\Sigma^{\varepsilon}_{\mathtt{CC}} \subset \Sigma_{\mathtt{C}}$: The current collector through which electrons enter (or leave) the conductive phase (*left boundary*)
- $\Sigma^{\varepsilon}_{\mathtt{EE}} \subset \Sigma_{\mathtt{E}}$: The bulk electrolyte through which ions enter (or leave) the electrolyte phase (*right boundary*)
- $\Sigma_{\mathtt{C}} \backslash \Sigma^{\varepsilon}_{\mathtt{CC}} =: \overline{\Sigma}^{\varepsilon}_{\mathtt{CC}}$: The electrolyte component of $\Sigma_{\mathtt{C}}$
- $\Sigma_{\mathtt{E}} \backslash \Sigma^{\varepsilon}_{\mathtt{EE}} =: \overline{\Sigma}^{\varepsilon}_{\mathtt{EE}}$: The conductive additive component of $\Sigma_{\mathtt{E}}$
- $\mathcal{S}_{\mathtt{AE}}$: The interface between $\mathcal{Z}_{\mathtt{A}}$ and $\mathcal{Z}_{\mathtt{E}}$ within $\mathcal{Z}$ (where the insertion reaction (81) occurs)
- $\mathcal{S}_{\mathtt{CE}}$: The interface between $\mathcal{Z}_{\mathtt{C}}$ and $\mathcal{Z}_{\mathtt{E}}$ within $\mathcal{Z}$ (no reactions)
- $\mathcal{S}_{\mathtt{AC}}$: The interface between $\mathcal{Z}_{\mathtt{C}}$ and $\mathcal{Z}_{\mathtt{A}}$ within $\mathcal{Z}$ (continuity of electron flux)
- $\mathcal{S}_{\mathtt{SE}} = \mathcal{S}_{\mathtt{CE}} \cup \mathcal{S}_{\mathtt{AE}}$:The interface between $\mathcal{Z}_{\mathtt{S}}$ and $\mathcal{Z}_{\mathtt{E}}$ within $\mathcal{Z}$

The corresponding repetitions of the interfaces are denoted by $\mathcal{S}^{\varepsilon}_{ij}$ and given by

$$\mathcal{S}^{\varepsilon}_{ij} = \varepsilon \mathcal{S}_{ij} + \varepsilon \mathbb{Z}^3 \,. \tag{147}$$

and global boundaries in Ω defined by the intersections

$$\Sigma^{\varepsilon}_{ij} = \Omega \cap \mathcal{S}^{\varepsilon}_{ij} \tag{148}$$

for the respective combinations of i and j.

Even though this geometry gives rise to the normal vectors $\mathbf{n}^{\varepsilon}_1$, $\mathbf{n}^{\varepsilon}_2$ we usually omit the index ε in this context.

5.2 The $\varepsilon-$ problem

Applying the geometric setup and the ε-definitions of the domains and interfaces to balance equations and boundary conditions derived in section 4.3 allows us to state compactly the following ε-problem. Note that we drop the superscripts $\hat{\cdot}$ of the pervious section for the variables, functions and parameters, for clarity and denote with $\mathbf{x}$ the non-dimensional space variable.

We have thus the following PDE system:

$$C_h \frac{\partial y_{\mathtt{A}_C}}{\partial t} = \varepsilon^2 \operatorname{div}\left(M_{\mathtt{A}} \nabla \mu_{\mathtt{A}}\right) \qquad \mathbf{x} \in \Omega^{\varepsilon}_{\mathtt{A}} \tag{149}$$

$$\mu_{\mathtt{A}} = f_{\mathtt{A}}(y_{\mathtt{A}}) - \gamma_{\mathtt{A}} \varepsilon^2 \operatorname{div} \nabla y_{\mathtt{A}} \qquad \mathbf{x} \in \Omega^{\varepsilon}_{\mathtt{A}} \tag{150}$$

$$0 = \operatorname{div}_{\xi}\left(\sigma_{\mathtt{S}}(\mathbf{x}) \nabla_{\xi} \varphi_{\mathtt{S}}\right) \qquad \mathbf{x} \in \Omega^{\varepsilon}_{\mathtt{S}} \tag{151}$$

$$C_h c_{\mathtt{E}} \frac{\partial y_{\mathtt{E}}}{\partial t} = \operatorname{div}\left(M^{\mathtt{E}}_{C,A} \nabla \mu_{\mathtt{E}_A} + M^{\mathtt{E}}_{C,C} \nabla \mu_{\mathtt{E}_C}\right) \qquad \mathbf{x} \in \Omega^{\varepsilon}_{\mathtt{E}} \tag{152}$$

$$C_h c_{\mathtt{E}} \frac{\partial y_{\mathtt{E}}}{\partial t} = \operatorname{div}\left(M^{\mathtt{E}}_{A,A} \nabla \mu_{\mathtt{E}_A} + M^{\mathtt{E}}_{A,C} \nabla \mu_{\mathtt{E}_C}\right) \qquad \mathbf{x} \in \Omega^{\varepsilon}_{\mathtt{E}} \tag{153}$$

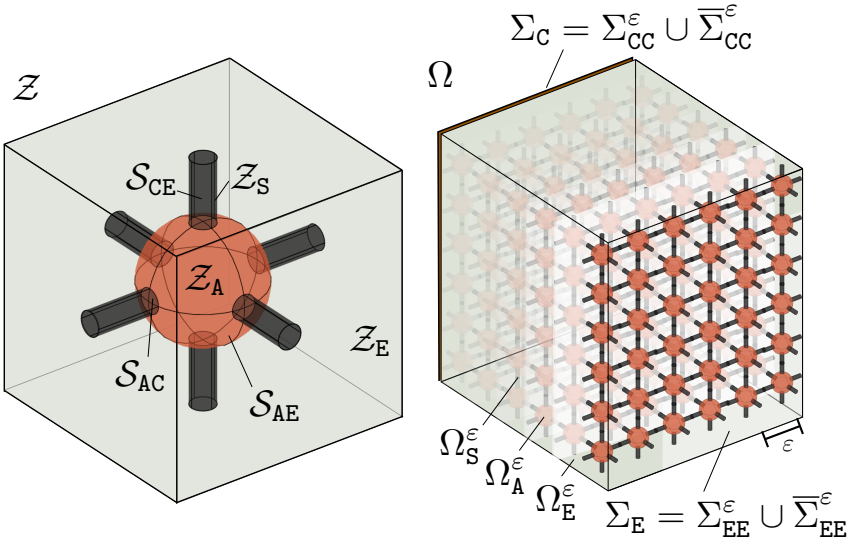

Figure 2: Left: $\mathcal{Z}$ split into $\mathcal{Z}_{\mathtt{A}}$ and $\mathcal{Z}_{\mathtt{E}} = Z \setminus \mathcal{Z}_{\mathtt{A}}$. Right: Ω split into the periodic parts $\Omega^{\varepsilon}_{\mathtt{A}}$ and Ω^{ε}_{E}.

or alternatively[6]

$$C_h c_{\mathtt{E}} \frac{\partial y_{\mathtt{E}}}{\partial t} = \operatorname{div}\left(D^y_{\mathtt{E}} \nabla y_{\mathtt{E}} + D^{\varphi}_{\mathtt{E}} \nabla \varphi_{\mathtt{E}}\right) \qquad \mathbf{x} \in \Omega^{\varepsilon}_{\mathtt{E}} \tag{154}$$

$$0 = \operatorname{div}\left(S_{\mathtt{E}} \nabla y_{\mathtt{E}} + \sigma_{\mathtt{E}} \nabla \varphi_{\mathtt{E}}\right) \qquad \mathbf{x} \in \Omega^{\varepsilon}_{\mathtt{E}}\,. \tag{155}$$

At the electrolyte-active phase interface we have the boundary conditions [7]

$$\varepsilon^2 \left(D_{\mathtt{A}} y_{\mathtt{A}}(1-y_{\mathtt{A}}) \nabla_\xi \mu_{\mathtt{A}}\right) \cdot \mathbf{n}_{\mathtt{A}} = \varepsilon^1 L \cdot g(\lambda) \qquad \text{on } \Sigma^{\varepsilon}_{\mathtt{AE}}\,, \tag{156}$$

$$\nabla y_{\mathtt{A}} \cdot \mathbf{n}_{\mathtt{A}} = 0 \qquad \text{on } \Sigma_{\mathtt{AE}}\,, \tag{157}$$

$$\left(\sigma_{\mathtt{S}}(\mathbf{x}) \nabla_\xi \varphi_{\mathtt{S}}\right) \cdot \mathbf{n}_{\mathtt{A}} = \varepsilon^1 L \cdot g(\lambda) \qquad \text{on } \Sigma^{\varepsilon}_{\mathtt{AE}}\,, \tag{158}$$

$$\left(D^y_{\mathtt{E}} \nabla y_{\mathtt{E}} + D^{\varphi}_{\mathtt{E}} \nabla \varphi_{\mathtt{E}}\right) \cdot \mathbf{n}_{\mathtt{E}} = -\varepsilon^1 L g(\lambda) \qquad \text{on } \Sigma^{\varepsilon}_{\mathtt{AE}}\,, \tag{159}$$

$$\left(S_{\mathtt{E}} \nabla y_{\mathtt{E}} + \sigma_{\mathtt{E}} \nabla \varphi_{\mathtt{E}}\right) \cdot \mathbf{n}_{\mathtt{E}} = -\varepsilon^1 L \cdot g(\lambda) \qquad \text{on } \Sigma^{\varepsilon}_{\mathtt{AE}}\,, \tag{160}$$

$$\lambda = -\left(\varphi_{\mathtt{S}} + \mu_{\mathtt{A}} - \varphi_{\mathtt{E}} - f_{\mathtt{E}}(y_{\mathtt{E}})\right) \qquad \text{on } \Sigma^{\varepsilon}_{\mathtt{AE}}\,, \tag{161}$$

with

$$g(\lambda) := \left(\mathrm{e}^{\alpha \cdot \lambda} - \mathrm{e}^{-(1-\alpha)\cdot \lambda}\right), \tag{162}$$

At the interface between the conductive additive and the active phase we have continuity of the solid charge flux, which is already considered in the formulation of (151) to hold for $\mathbf{x} \in \Omega^{\varepsilon}_{\mathtt{S}}$, as well as no-flux boundary conditions

$$\varepsilon^2 \left(\nabla_\xi \mu_{\mathtt{A}}\right) \cdot \mathbf{n} = 0 \qquad \text{on } \Sigma^{\varepsilon}_{\mathtt{AC}}\,, \tag{163}$$

$$\nabla y_{\mathtt{A}} \cdot \mathbf{n} = 0 \qquad \text{on } \Sigma^{\varepsilon}_{\mathtt{AC}}\,. \tag{164}$$

The electrolyte-conductive additive interface is considered to be inert, whereby we have the no-flux boundary conditions

[6] Note, we discuss the homogenization of the electrolyte equations on the basis of (152) and (153), because we know $(M^{\mathtt{E}}_{\alpha,\beta})_{\alpha,\beta})$ is symmetric and positive semi-definite, and apply then the homogenization result to (154) and (155), since they are equivalent in the electro-neutral case.

[7] Note that $\mathbf{n}_{\mathtt{A}}$ is pointing from the $Z_{\mathtt{A}}$ into $Z_{\mathtt{E}}$ and $\mathbf{n}_{\mathtt{E}}$ from $Z_{\mathtt{E}}$ into $Z_{\mathtt{A}}$, with $\mathbf{n}_{\mathtt{A}} = -\mathbf{n}_{\mathtt{E}}$. If no index for $\mathbf{n}$ is given, $\mathbf{n}$ denotes always the outward unit normal vector and it is clear from the the context.

$$\big(D_{\mathtt{E}}^{y}\nabla y_{\mathtt{E}} + D_{\mathtt{E}}^{\varphi}\nabla\varphi_{\mathtt{E}}\big)\cdot\mathbf{n} = 0 \qquad \text{on } \Sigma_{\mathtt{AC}}^{\varepsilon}\,, \tag{165}$$

$$\big(S_{\mathtt{E}}\nabla y_{\mathtt{E}} + \sigma_{\mathtt{E}}\nabla\varphi_{\mathtt{E}}\big)\cdot\mathbf{n} = 0 \qquad \text{on } \Sigma_{\mathtt{AC}}^{\varepsilon}\,. \tag{166}$$

On the *left side* of the porous electrode, we have electrical current flux boundary condition

$$\big(\sigma_{\mathtt{S}}(\mathbf{x})\nabla_{\xi}\varphi_{\mathtt{S}}\big)\cdot\mathbf{n} = \psi_{\mathtt{A}}\cdot i(t)C_h \qquad \text{on } \Sigma_{\mathtt{CC}}^{\varepsilon} \tag{167}$$

as well as the no-flux boundary conditions for the electrolyte species, i.e.

$$\big(D_{\mathtt{E}}^{y}\nabla y_{\mathtt{E}} + D_{\mathtt{E}}^{\varphi}\nabla\varphi_{\mathtt{E}}\big)\cdot\mathbf{n} = 0 \qquad \text{on } \overline{\Sigma}_{\mathtt{CC}}^{\varepsilon}\,, \tag{168}$$

$$\big(S_{\mathtt{E}}\nabla y_{\mathtt{E}} + \sigma_{\mathtt{E}}\nabla\varphi_{\mathtt{E}}\big)\cdot\mathbf{n} = 0 \qquad \text{on } \overline{\Sigma}_{\mathtt{CC}}^{\varepsilon}\,. \tag{169}$$

On the *right side* of the porous electrode, we have fix the electrolyte concentration and the electrostatic potential, i.e.

$$\varphi_{\mathtt{E}} = \varphi_{\mathtt{E}}^{\mathsf{init}} \qquad \text{on } \Sigma_{\mathtt{EE}}^{\varepsilon} \tag{170}$$

$$y_{\mathtt{E}} = \varphi_{\mathtt{E}}^{\mathsf{init}} \qquad \text{on } \Sigma_{\mathtt{EE}}^{\varepsilon} \tag{171}$$

and have in addition no-flux boundary conditions for the solid phase electrical current:

$$\big(\sigma_{\mathtt{S}}(\mathbf{x})\nabla_{\xi}\varphi_{\mathtt{S}}\big)\cdot\mathbf{n} = 0 \qquad \text{on } \overline{\Sigma}_{\mathtt{EE}}^{\varepsilon}\,. \tag{172}$$

The initial values are considered as

$$y_{\mathtt{A}}(\mathbf{x}, t=0) = y_{\mathtt{A}}^{\mathsf{init}}(=\text{const.}) \qquad \mathbf{x}\in\Omega_{\mathtt{A}}^{\varepsilon} \tag{173}$$

$$y_{\mathtt{E}}(\mathbf{x}, t=0) = y_{\mathtt{E}}^{\mathsf{init}}(=\text{const.}) \qquad \mathbf{x}\in\Omega_{\mathtt{E}}^{\varepsilon} \tag{174}$$

$$\varphi_{\mathtt{E}}(\mathbf{x}, t=0) = 0 \qquad \mathbf{x}\in\Omega_{\mathtt{E}}^{\varepsilon} \tag{175}$$

$$\varphi_{\mathtt{S}}(\mathbf{x}, t=0) = 0 \qquad \mathbf{x}\in\Omega_{\mathtt{S}}^{\varepsilon}\,, \tag{176}$$

Note that

$$f_{\mathtt{A}}(y_{\mathtt{A}}^{\mathsf{init}}) = 0 \qquad \text{and} \qquad f_{\mathtt{E}}(y_{\mathtt{E}}^{\mathsf{init}}) = 0 \tag{177}$$

due to the re-scaling of $f_{\mathtt{A}}$ and $f_{\mathtt{E}}$, (c.f. section 4.3.1) whereby

$$\mu_{\mathtt{A}}(\mathbf{x}, t=0) = 0 \qquad \mathbf{x}\in\Omega_{\mathtt{A}}^{\varepsilon}\,. \tag{178}$$

and at $t=0$ we have

$$\lambda = 0 \qquad \text{on } \Sigma_{\mathtt{AE}}^{\varepsilon}\,. \tag{179}$$

5.3 Asymptotic Expansion

We will use asymptotic expansion in equations (149)–(155) to derive homogenized balance equations in the slow and fast charging regimes, respectively. For this, we consider the asymptotic expansion of the variables

$$\{y_{\mathtt{E}}^{\varepsilon}(x),\quad \varphi_{\mathtt{E}}^{\varepsilon}(x),\quad \varphi_{\mathtt{S}}(x),\quad y_{\mathtt{A}}^{\epsilon}(x)/\mu_{\mathtt{A}}^{\varepsilon}(x)\} =: \mathcal{I}$$

in the form ($u^\varepsilon \in \mathcal{I}$):

$$u^\varepsilon(x) = u^0(x,z) + \varepsilon\, u^1(x,z) + \varepsilon^2\, u^2(x,z) + \cdots\,, \tag{180}$$

where

$$z = \frac{x}{\varepsilon}$$

is the (oscillating) micro-scale variable and x the macro-scale variable. The functions $u^k(x,z)$ are defined on $\Omega \times \mathcal{Z}$ and are periodic in z with respect to the unit cell of periodicity $\mathcal{Z}$. For the differential operators, we have

$$\operatorname{div} \;\to\; \operatorname{div}_x + \varepsilon^{-1} \operatorname{div}_z, \qquad \nabla \to \nabla_x + \varepsilon^{-1}\nabla_z \quad \text{and} \tag{181}$$

where $\operatorname{div}_x, \nabla_x$ acts on the macro-scale variable x and $\operatorname{div}_z, \nabla_z$ on the micro-scale z.

We seek in general the balance equations for the leading order terms u^0 and truncate the series expansions of u after the u^1-term for simplicity.

The time-derivative yields

$$\partial_t u^\varepsilon = \partial_t u^0 + \varepsilon \partial_t u^1 + \mathcal{O}(\varepsilon^2) \tag{182}$$

and for non-linear functions $h = h(u)$ we consider the $\varepsilon-$Taylor expansion

$$h(u) = h(u^0) + \varepsilon u^1 h'(u^0) + \mathcal{O}(\varepsilon^2)\,. \tag{183}$$

For functions $g = g(u_{\mathtt{E}}, u_{\mathtt{A}})$ at some interface[8] Σ, we consider the multi-dimensional Taylor expansion in ε, *i.e.*

$$g(u_{\mathtt{E}}, u_{\mathtt{A}}) = g(u^0_{\mathtt{E}}, u^0_{\mathtt{A}}) + \varepsilon \partial_{u_{\mathtt{E}}} g\big|_{u^0_{\mathtt{E}}, u^0_{\mathtt{A}}} u^1_{\mathtt{E}} + \varepsilon \partial_{u_{\mathtt{A}}} g\big|_{u^0_{\mathtt{E}}, u^0_{\mathtt{A}}} u^1_{\mathtt{A}} + \mathcal{O}(\varepsilon^2). \tag{184}$$

Further, for $\operatorname{div}(D(u)\nabla u^\varepsilon)$ we have the expansion

$$\begin{aligned}\operatorname{div}(D(u)\nabla u^\varepsilon) = \varepsilon^{-2}&\Big[\operatorname{div}_z(D(u^0)\nabla_z u^0)\Big] \\ +\varepsilon^{-1}&\Big[\operatorname{div}_x(D(u^0)\nabla_z u^0) + \operatorname{div}_z(D(u^0)\nabla_x u^0) + \operatorname{div}_z(D(u^0)\nabla_z u^1)\Big] \\ +\varepsilon^{0}&\Big[\operatorname{div}_x(D(u^0)\nabla_x u^0) + \operatorname{div}_x(D(u^0)\nabla_z u^1) + \operatorname{div}_z(D(u^0)\nabla_x u^1)\Big] + \mathcal{O}(\varepsilon)\end{aligned} \tag{185}$$

and at some boundary for $(D(u)\nabla u^\varepsilon)\cdot \mathbf{n}$ the expansion

$$\begin{aligned}(D(u)\nabla u^\varepsilon)\cdot\mathbf{n} = \varepsilon^{-1}&\Big[(D(u^0)\nabla_z u^0)\cdot\mathbf{n}\Big] + \varepsilon^0\Big[(D(u^0)\nabla_x u^0 + D(u^0)\nabla_z u^1)\cdot\mathbf{n}\Big] \\ +\varepsilon^1&\Big[(D(u^0)\nabla_x u^1)\cdot\mathbf{n}\Big] + \mathcal{O}(\varepsilon^2)\,.\end{aligned} \tag{186}$$

[8] Note that $u_{\mathtt{E}}$ refers here to the evaluation of $u_{\mathtt{E}}$ at the interface Σ on the electrolyte side $\Omega_{\mathtt{E}}$, *i.e.* , while $u_{\mathtt{A}}$ denotes the evaluation on Σ on the active phase side $\Omega_{\mathtt{A}}$.

6 Homogenization of a Porous Electrode with multiple phase transitions

We study now the asymptotic expansion for the charging regime of finite C-rates C_h, where open circuit voltage conditions can be obtained for $C_h \to 0$. We will first study eq. (151) as it is not only an important case study for the combined expansion of (152)–(153) but will be crucial for the understanding of the slow charging as well. We then apply expansion to (154)–(155) and finally to (149) which are summarized in the paragraph 7.1.

6.1 Solid Phase: Expansion of (151)

We study the multi-scale expansions for

$$
\begin{aligned}
0 = \operatorname{div}\left(\sigma_{\mathtt{S}}(\mathbf{x})\nabla\varphi_{\mathtt{S}}^{\varepsilon}\right) &\qquad \text{in } \Omega_{\mathtt{S}}^{\varepsilon}\,, &(187)\\
\left(\sigma_{\mathtt{S}}(\mathbf{x})\nabla\varphi_{\mathtt{S}}^{\varepsilon}\right)\cdot\mathbf{n} = \varepsilon^{1} L\cdot g\left(\lambda^{\varepsilon}\right) &\qquad \text{on } \Sigma_{\mathtt{AE}}^{\varepsilon}\,, &(188)\\
\left(\sigma_{\mathtt{S}}(\mathbf{x})\nabla\varphi_{\mathtt{S}}^{\varepsilon}\right)\cdot\mathbf{n} = 0 &\qquad \text{on } \Sigma_{\mathtt{CE}}^{\varepsilon}\,, &(189)\\
\left(\sigma_{\mathtt{S}}(\mathbf{x})\nabla\varphi_{\mathtt{S}}^{\varepsilon}\right)\cdot\mathbf{n} = \psi_{\mathtt{A}} i(t) C_h &\qquad \text{on } \Sigma_{\mathtt{CC}}^{\varepsilon} &(190)\\
\left(\sigma_{\mathtt{S}}(\mathbf{x})\nabla\varphi_{\mathtt{S}}^{\varepsilon}\right)\cdot\mathbf{n} = 0 &\qquad \text{on } \overline{\Sigma}_{\mathtt{EE}}^{\varepsilon}\,. &(191)
\end{aligned}
$$

with ($\mathcal{Z}_{\mathtt{S}} = \mathcal{Z}_{\mathtt{A}} \cup \mathcal{Z}_{\mathtt{C}}$) and

$$
\sigma_{\mathtt{S}} = \sigma_{\mathtt{S}}^{0}\cdot\eta_{\mathtt{S}}(\frac{\mathbf{x}}{\varepsilon})\,, \qquad \eta_{\mathtt{S}}(z) = \begin{cases} 1 & z\in\mathcal{Z}_{\mathtt{C}} \\ \frac{\sigma_{\mathtt{A}}^{0}}{\sigma_{\mathtt{S}}^{0}} & z\in\mathcal{Z}_{\mathtt{A}}\,. \end{cases} \tag{192}
$$

Order ε^{-2}:

$$
\begin{aligned}
\operatorname{div}_z\Big(\sigma_{\mathtt{S}}(x)\nabla_z\varphi_{\mathtt{S}}^{0}\Big) = 0 &\qquad \text{on } \Omega\times\mathcal{Z}_{\mathtt{S}}\,,\\
(\sigma_{\mathtt{S}}(x)\nabla_z\varphi_{\mathtt{S}}^{0}(x,z))\cdot\mathbf{n} = 0 &\qquad \text{on } \Omega\times\mathcal{S}_{\mathtt{SE}}\,.
\end{aligned}
$$

which implies the condition $\nabla_z\varphi_{\mathtt{S}}^{0} = 0$ since $\sigma_{\mathtt{S}} > 0$, i.e. $\varphi_{\mathtt{S}}^{0}$ is constant w.r.t. the micro-scale variable z.

Order ε^{-1}: We make use of $\nabla_z\varphi_{\mathtt{S}}^{0} = 0$ and obtain

$$
\begin{aligned}
\operatorname{div}_z\Big(\sigma_{\mathtt{S}}^{0}\eta_{\mathtt{S}}(z)\nabla_x\varphi_{\mathtt{S}}^{0} + \sigma_{\mathtt{S}}(x)\nabla_z\varphi_{\mathtt{S}}^{1}\Big) = 0 &\qquad \text{on } \Omega\times\mathcal{Z}_{\mathtt{S}}\,, &(193)\\
\sigma_{\mathtt{S}}^{0}\eta_{\mathtt{S}}(z)\Big(\nabla_x\varphi_{\mathtt{S}}^{0}(x) + \nabla_z\varphi_{\mathtt{S}}^{1}(x,z)\Big)\cdot\mathbf{n} = 0, &\qquad \text{on } \Omega\times\mathcal{S}_{\mathtt{SE}}\,. &(194)\\
\sigma_{\mathtt{S}}^{0}\eta_{\mathtt{S}}(z)\Big(\nabla_x\varphi_{\mathtt{S}}^{0}(x) + \nabla_z\varphi_{\mathtt{S}}^{1}(x,z)\Big)\cdot\mathbf{n} = i(t)C_h\cdot\psi_{\mathtt{A}} &\qquad \text{on } \Sigma_{\mathtt{C}}\times\mathcal{Z}_{\mathtt{S}} &(195)\\
\sigma_{\mathtt{S}}^{0}\eta_{\mathtt{S}}(z)\Big(\nabla_x\varphi_{\mathtt{S}}^{0}(x) + \nabla_z\varphi_{\mathtt{S}}^{1}(x,z)\Big)\cdot\mathbf{n} = 0 &\qquad \text{on } \Sigma_{\mathtt{E}}\times\mathcal{Z}_{\mathtt{S}} &(196)
\end{aligned}
$$

Now, let the functions $\chi_{\mathtt{S},i}(z), i = 1,2,3$, satisfy the cell problem

$$
\mathbf{CP}-\mathcal{Z}_{\mathtt{S}}: \begin{cases} \operatorname{div}_z\Big(\eta_{\mathtt{S}}(z)\Big(e_i + \nabla_z\chi_{\mathtt{S},i}(z)\Big)\Big) = 0 & \text{in } \mathcal{Z}_{\mathtt{S}} \\ \eta_{\mathtt{S}}(z)\Big(e_i + \nabla_z\chi_{\mathtt{S},i}(z)\Big)\cdot\mathbf{n} = 0 & \text{on } \mathcal{S}_{\mathtt{SE}}\ . \\ \chi_{\mathtt{S},i}(z)\ \text{ is }\ \mathcal{Z}_{\mathtt{S}}\text{- periodic} \end{cases} \tag{197}
$$

Then we can verify that

$$\varphi_{\mathtt{S}}^1(x,z) = -\boldsymbol{\chi}_{\mathtt{S}}(z) \cdot \nabla_x \varphi_{\mathtt{S}}^0(x)\,, \tag{198}$$

where $\boldsymbol{\chi}_{\mathtt{S}} = (\chi_{\mathtt{S},1}, \chi_{\mathtt{S},2}, \chi_{\mathtt{S},3})$ solves the order -1 problem for a given $\varphi_{\mathtt{S}}^0$.

The macro-scale boundary condition (195) thus reads

$$\sigma_{\mathtt{S}}^0 \eta_{\mathtt{S}}(z)\Big(\mathbf{Id} - \nabla_z \boldsymbol{\chi}_{\mathtt{S}}\Big)\nabla_x \varphi_{\mathtt{S}}^0(x)\cdot \mathbf{n} = i(t) C_h \psi_{\mathtt{A}} \qquad \text{on } \Sigma_{\mathtt{C}} \times \mathcal{Z}_{\mathtt{S}}\,, \tag{199}$$

$$\sigma_{\mathtt{S}}^0 \eta_{\mathtt{S}}(z)\Big(\mathbf{Id} - \nabla_z \boldsymbol{\chi}_{\mathtt{S}}\Big)\nabla_x \varphi_{\mathtt{S}}^0(x)\cdot \mathbf{n} = 0 \qquad \text{on } \Sigma_{\mathtt{E}} \times \mathcal{Z}_{\mathtt{S}}\,. \tag{200}$$

Order ε^0: Insertion of $\varphi_{\mathtt{S}}^1(x,z) = -\boldsymbol{\chi}_{\mathtt{S}}(z) \cdot \nabla_x \varphi_{\mathtt{S}}^0(x)$ yields

$$\begin{aligned} \operatorname{div}_x\Big(\sigma_{\mathtt{S}}^0 \eta_{\mathtt{S}}(z)\big(\mathbf{Id} - \nabla_z \boldsymbol{\chi}_{\mathtt{S}}\big)\cdot \nabla_x \varphi_{\mathtt{S}}^0\Big) + \operatorname{div}_z\Big(\sigma_{\mathtt{S}}^0 \eta_{\mathtt{S}}(z)\nabla_x \varphi_{\mathtt{S}}^1\Big) &= 0 && \text{on } \Omega \times \mathcal{Z}_{\mathtt{S}}\,,\\ \sigma_{\mathtt{S}}^0 \eta_{\mathtt{S}}(z)\nabla_x \varphi_{\mathtt{S}}^1 \cdot \mathbf{n} &= L g(\lambda^0) && \text{on } \Omega \times \mathcal{S}_{\mathtt{AE}}\\ \sigma_{\mathtt{S}}^0 \eta_{\mathtt{S}}(z)\nabla_x \varphi_{\mathtt{S}}^1 \cdot \mathbf{n} &= 0 && \text{on } \Omega \times \mathcal{S}_{\mathtt{CE}} \end{aligned}$$

with

$$\lambda^0 = -\big(\varphi_{\mathtt{S}}^0 + \mu_{\mathtt{A}}^0|_{\mathcal{S}_{\mathtt{AE}}} - \varphi_{\mathtt{E}}^0 - f_{\mathtt{E}}(y_{\mathtt{E}}^0)\big) \qquad \text{on } \Omega \times \mathcal{S}_{\mathtt{AE}}\,. \tag{201}$$

An integration over $\mathcal{Z}_{\mathtt{S}}$ yields thus [9]

$$\operatorname{div}_x \cdot \big(\sigma_{\mathtt{S}}^0 \boldsymbol{\pi}_{\mathtt{S}} \nabla_x \varphi_{\mathtt{S}}^0\big) + \frac{\theta_{\mathtt{AE}}}{\psi_{\mathtt{A}}} \fint_{\mathcal{S}_{\mathtt{AE}}} L\, g(\lambda^0) dA = 0 \qquad \text{in } \Omega \tag{202}$$

$$\sigma_{\mathtt{S}}^0 \boldsymbol{\pi}_{\mathtt{S}} \nabla_x \varphi_{\mathtt{S}}^0(x)\cdot \mathbf{n} = i(t) C_h \qquad \text{on } \Sigma_{\mathtt{C}} \tag{203}$$

$$\sigma_{\mathtt{S}}^0 \boldsymbol{\pi}_{\mathtt{S}} \nabla_x \varphi_{\mathtt{S}}^0(x)\cdot \mathbf{n} = 0 \qquad \text{on } \Sigma_{\mathtt{E}}\,. \tag{204}$$

with

$$\fint_{\mathcal{S}_{\mathtt{AE}}} L\, g(\lambda^0) dA := \frac{1}{\int_{\mathcal{S}_{\mathtt{AE}}} 1 dA(z)} \int_{\mathcal{S}_{\mathtt{AE}}} L\, g(\lambda^0) dA(z) \tag{205}$$

and [10]

$$\psi_{\mathtt{A}} := \int_{\mathcal{Z}_{\mathtt{A}}} 1 dV(z)\,,\ \boldsymbol{\pi}_{\mathtt{S}} := \frac{1}{\psi_{\mathtt{A}}} \int_{\mathcal{Z}_{\mathtt{S}}} \eta_{\mathtt{S}}(z)(\mathbf{Id} - \nabla_z \boldsymbol{\chi}_{\mathtt{S}})\, dV(z)\,,\ \theta_{\mathtt{AE}} := \int_{\mathcal{S}_{\mathtt{AE}}} 1\, dA(z) \tag{206}$$

where $\psi_{\mathtt{A}}$ is called volume fraction of the active phase $\Omega_{\mathtt{A}}$, $\boldsymbol{\pi}_{\mathtt{S}}$ the (diffusional) corrector, and $\theta_{\mathtt{AE}}$ the specific interfacial area of the interface $\mathcal{S}_{\mathtt{AE}}$. The corrector function $\boldsymbol{\chi}_{\mathtt{S}}$ is determined from **CP** - $\mathcal{Z}_{\mathtt{S}}$ (eq. (197)).

Note that quite frequently a spherical symmetry is assumed on the micro-scale. For our considered geometry (c.f. Figure 2) this is certainly an approximation as the conductive additives in general break the spherical symmetry.

[9] Note that indeed a division by $\psi_{\mathtt{A}}$ is done, and not by $\psi_{\mathtt{S}}$, because the current is supposed to scale with the amount of active material $\psi_{\mathtt{A}}$.

[10] Note that we set vol$\{\mathcal{Z}\} = 1$.

6.2 Electrolyte

6.2.1 Expansion of (152)– (153)

We now redo the the calculations of section 6.1 in the context of (152)– (153) with its corresponding boundary conditions. Since the two equations involve cross-diffusion between $y_{\mathtt{E}}^\varepsilon$ and $\varphi_{\mathtt{E}}^\varepsilon$ we have to handle them both at once.

The derivation of the homogenized equation system is more convenient in the thermodynamic representation (152)– (153) since we need to exploit the positive semi-definintess of the mobility matrix. Below, in paragraph 6.2.2 we apply the result of this section to eqs. (154)– (155) in order to obtain the homogenized balance equations of the electrolyte phase.

Consider thus

$$\partial_t y_1^\varepsilon = \operatorname{div}(M_{11}\nabla\mu_1^\varepsilon + M_{12}\nabla\mu_2^\varepsilon) \qquad \text{in } \Omega_{\mathtt{E}}^\varepsilon\,, \tag{207}$$
$$\partial_t y_2^\varepsilon = \operatorname{div}(M_{12}\nabla\mu_1^\varepsilon + M_{22}\nabla\mu_2^\varepsilon) \qquad \text{in } \Omega_{\mathtt{E}}^\varepsilon\,, \tag{208}$$
$$\tag{209}$$

with boundary conditions[11]

$$(M_{11}\nabla\mu_1^\varepsilon + M_{12}\nabla\mu_2^\varepsilon)\cdot\mathbf{n} = -\varepsilon \underset{s}{R}_1^\varepsilon \qquad \text{on } \Sigma_{\mathtt{AE}}^\varepsilon \tag{210}$$
$$(M_{11}\nabla\mu_1^\varepsilon + M_{12}\nabla\mu_2^\varepsilon)\cdot\mathbf{n} = 0 \qquad \text{on } \Sigma_{\mathtt{CE}}^\varepsilon \tag{211}$$
$$(M_{12}\nabla\mu_1^\varepsilon + M_{22}\nabla\mu_2^\varepsilon)\cdot\mathbf{n} = 0 \qquad \text{on } \Sigma_{\mathtt{SE}}^\varepsilon \tag{212}$$
$$\frac{1}{2}(\mu_1^\varepsilon - \mu_2^\varepsilon) = \varphi_{\mathtt{E}}^{\mathsf{init}} \qquad \text{on } \Sigma_{\mathtt{EE}}^\varepsilon \tag{213}$$
$$\frac{1}{2}(\mu_1^\varepsilon + \mu_2^\varepsilon) = f_{\mathtt{E}}(y_{\mathtt{E}}^{\mathsf{init}}) \qquad \text{on } \Sigma_{\mathtt{EE}}^\varepsilon \tag{214}$$
$$(M_{11}\nabla\mu_1^\varepsilon + M_{12}\nabla\mu_2^\varepsilon)\cdot\mathbf{n} = 0 \qquad \text{on } \overline{\Sigma}_{\mathtt{CC}}^\varepsilon \tag{215}$$
$$(M_{12}\nabla\mu_1^\varepsilon + M_{22}\nabla\mu_2^\varepsilon)\cdot\mathbf{n} = 0 \qquad \text{on } \overline{\Sigma}_{\mathtt{CC}}^\varepsilon \tag{216}$$

and ($i = 1, 2$)

$$\mu_i = f_{\mathtt{E}}(y_{\mathtt{E}}) - (-1)^i\varphi_{\mathtt{E}} \tag{217}$$

with a strictly monotonic function $f_{\mathtt{E}}$.

This yields the following in orders of ε:

Order ε^{-2}:

$$\operatorname{div}_z(M_{11}\nabla_z\mu_1^0 + M_{12}\nabla_z\mu_2^0) = 0 \qquad \text{on } \Omega\times\mathcal{Z}_{\mathtt{E}}\,, \tag{218}$$
$$\operatorname{div}_z(M_{12}\nabla_z\mu_1^0 + M_{22}\nabla_z\mu_2^0) = 0 \qquad \text{on } \Omega\times\mathcal{Z}_{\mathtt{E}} \tag{219}$$

[11] $\mathbf{n}$ denotes the outward unit vector.

with

$$(M_{11}\nabla_z\mu_1^0 + M_{12}\nabla_z\mu_2^0)\cdot\mathbf{n} = 0 \qquad \text{on } \Omega\times\mathcal{S}_{\mathtt{SE}}\,, \tag{220}$$
$$(M_{12}\nabla_z\mu_1^0 + M_{22}\nabla_z\mu_2^0)\cdot\mathbf{n} = 0 \qquad \text{on } \Omega\times\mathcal{S}_{\mathtt{SE}}\,, \tag{221}$$

yielding

$$\nabla_z\mu_1^0 = 0, \qquad \nabla_z\mu_2^0 = 0 \tag{222}$$

since (M_{ij}) is positive semi-definite. Hence, we can conclude $\mu_i^0 =$ const. and thus $y_{\mathtt{E}}^0 =$ const. and $\varphi_{\mathtt{E}}^0 =$ const. w.r.t. to z, respectively.

Order ε^{-1}: Exploiting $\nabla_z\mu_1^0 = 0$ and $\nabla_z\mu_2^0 = 0$ yields

$$\mathrm{div}_z(M_{11}\nabla_z\mu_1^1 + M_{12}\nabla_z\mu_2^1 + M_{11}\nabla_x\mu_1^0 + M_{12}\nabla_x\mu_2^0) = 0 \qquad \text{on } \Omega\times\mathcal{Z}_{\mathtt{E}}\,, \tag{223}$$
$$\mathrm{div}_z(M_{12}\nabla_z\mu_1^1 + M_{22}\nabla_z\mu_2^1 + M_{12}\nabla_x\mu_1^0 + M_{22}\nabla_x\mu_2^0) = 0 \qquad \text{on } \Omega\times\mathcal{Z}_{\mathtt{E}}\,, \tag{224}$$

with boundary conditions

$$(M_{11}\nabla_z\mu_1^1 + M_{12}\nabla_z\mu_2^1 + M_{11}\nabla_x\mu_1^0 + M_{12}\nabla_x\mu_2^0)\cdot\mathbf{n} = 0 \qquad \text{on } \Omega\times\mathcal{S}_{\mathtt{SE}}\,, \tag{225}$$
$$(M_{12}\nabla_z\mu_1^1 + M_{22}\nabla_z\mu_2^1 + M_{12}\nabla_x\mu_1^0 + M_{22}\nabla_x\mu_2^0)\cdot\mathbf{n} = 0 \qquad \text{on } \Omega\times\mathcal{S}_{\mathtt{SE}}\,. \tag{226}$$

We expect

$$\mu_1^1 = -\boldsymbol{\chi}_{11}\nabla_x\mu_1^0 - \boldsymbol{\chi}_{12}\nabla_x\mu_2^0 \qquad \text{on } \Omega\times\mathcal{Z}_{\mathtt{E}}\,, \tag{227}$$
$$\mu_2^1 = -\boldsymbol{\chi}_{21}\nabla_x\mu_1^0 - \boldsymbol{\chi}_{22}\nabla_x\mu_2^0 \qquad \text{on } \Omega\times\mathcal{Z}_{\mathtt{E}}\,, \tag{228}$$

i.e. a micro-scale intercalation between μ_1^0 and μ_2^0 propagating into μ_1^1 and μ_2^1.

However, **if** the $M_{\alpha\beta}$ are constant in space (but might depend on (u_1^0, u_2^0) we show in appendix A that

$$\boldsymbol{\chi}_{12} = \mathbf{0} \tag{229}$$
$$\boldsymbol{\chi}_{11} = \boldsymbol{\chi}_{22} =: \boldsymbol{\chi}_{\mathtt{E}} \tag{230}$$

where $\boldsymbol{\chi}_{\mathtt{E}} = (\chi_{\mathtt{E},1}(z), \chi_{\mathtt{E},2}(z), \chi_{\mathtt{E},3}(z))^T$ solves the cell problem ($i = 1, 2, 3$)

$$\textbf{CP}-\mathcal{Z}_{\mathtt{E}}: \begin{cases} \mathrm{div}_z(\nabla\boldsymbol{\chi}_{\mathtt{E},i}) = 0 & \text{in } \mathcal{Z}_{\mathtt{E}} \\ \Big(e_i + \nabla_z\chi_{\mathtt{E},i}(z)\Big)\cdot\mathbf{n} = 0 & \text{on } \mathcal{S}_{\mathtt{SE}} \\ \chi_{\mathtt{E},i}(z) \text{ is } \mathcal{Z}_{\mathtt{E}}\text{ - periodic} & \end{cases}. \tag{231}$$

For the macro-scale boundary conditions we obtain thus

$$\Big(M_{11}(\mathbf{Id} - \nabla_z\boldsymbol{\chi}_{\mathtt{E}})\nabla_x\mu_1^0 + M_{12}(\mathbf{Id} - \nabla_z\boldsymbol{\chi}_{\mathtt{E}})\nabla_x\mu_2^0\Big)\cdot\mathbf{n} = 0 \qquad \text{on } \Sigma_{\mathtt{C}}\times\mathcal{Z}_{\mathtt{E}} \tag{232}$$
$$\Big(M_{12}(\mathbf{Id} - \nabla_z\boldsymbol{\chi}_{\mathtt{E}})\nabla_x\mu_1^0 + M_{22}(\mathbf{Id} - \nabla_z\boldsymbol{\chi}_{\mathtt{E}})\nabla_x\mu_2^0\Big)\cdot\mathbf{n} = 0 \qquad \text{on } \Sigma_{\mathtt{C}}\times\mathcal{Z}_{\mathtt{E}} \tag{233}$$

Order ε^0: In leading order we obtain thus

$$\begin{aligned}\partial_t u_1^0 =&\ \operatorname{div}_x(M_{11}\nabla_x\mu_1^0 + M_{12}\nabla_x\mu_2^0 + M_{11}\nabla_z\mu_1^1 + M_{12}\nabla_z\mu_2^1)\\ &+ \operatorname{div}_z(M_{11}\nabla_x\mu_1^1 + M_{12}\nabla_x\mu_2^1) \qquad \text{on } \Omega\times\mathcal{Z}_{\mathtt{E}} \qquad (234)\\ \partial_t u_2^0 =&\ \operatorname{div}_x(M_{12}\nabla_x\mu_1^0 + M_{22}\nabla_x\mu_2^0 + M_{12}\nabla_z\mu_1^1 + M_{22}\nabla_z\mu_2^1)\\ &+ \operatorname{div}_z(M_{12}\nabla_x\mu_1^1 + M_{22}\nabla_x\mu_2^1) \qquad \text{on } \Omega\times\mathcal{Z}_{\mathtt{E}} \qquad (235)\end{aligned}$$

with boundary conditions

$$\begin{aligned}(M_{11}\nabla\mu_1^1 + M_{12}\nabla\mu_2^1)\cdot\mathbf{n} &= -\overset{0}{\underset{s}{R}}_1^0 \qquad \text{on } \Omega\times\mathcal{S}_{\mathtt{AE}} \qquad (236)\\ (M_{11}\nabla\mu_1^1 + M_{12}\nabla\mu_2^1)\cdot\mathbf{n} &= 0 \qquad \text{on } \Omega\times\mathcal{S}_{\mathtt{CE}} \qquad (237)\\ (M_{12}\nabla\mu_1^1 + M_{22}\nabla\mu_2^1)\cdot\mathbf{n} &= 0 \qquad \text{on } \Omega\times\mathcal{S}_{\mathtt{SE}} \qquad (238)\end{aligned}$$

An insertion of

$$\begin{aligned}\mu_1^1 &= -\boldsymbol{\chi}_{\mathtt{E}}\cdot\nabla_x\mu_1^0 \qquad (239)\\ \mu_2^1 &= -\boldsymbol{\chi}_{\mathtt{E}}\cdot\nabla_x\mu_2^0 \qquad (240)\end{aligned}$$

with subsequent integration over $\mathcal{Z}_{\mathtt{E}}$ thus yields

$$\begin{aligned}\partial_t u_1^0 =&\ \operatorname{div}_x\left(\boldsymbol{\pi}_{\mathtt{E}}\big(M_{11}\nabla_x\mu_1^0 + M_{12}\nabla_x\mu_2^0\big)\right) - \frac{\theta_{\mathtt{AE}}}{\psi_{\mathtt{E}}}\fint_{\mathcal{S}_{\mathtt{AE}}}\overset{0}{\underset{s}{R}}_1^0 dA \qquad \text{on } \Omega \qquad (241)\\ \partial_t u_2^0 =&\ \operatorname{div}_x\left(\boldsymbol{\pi}_{\mathtt{E}}\big(M_{12}\nabla_x\mu_1^0 + M_{22}\nabla_x\mu_2^0\big)\right) \qquad \text{on } \Omega \qquad (242)\end{aligned}$$

with

$$\fint_{\mathcal{S}_{\mathtt{AE}}}\overset{0}{\underset{s}{R}}_1^0 dA := \frac{1}{\int_{\mathcal{S}_{\mathtt{AE}}}1dA}\int_{\mathcal{S}_{\mathtt{AE}}}\overset{0}{\underset{s}{R}}_1^0 dA\,. \qquad (243)$$

and

$$\psi_{\mathtt{E}} := \int_{\mathcal{Z}_{\mathtt{E}}}1dV(z)\,,\quad \theta_{\mathtt{AE}} = \int_{\mathcal{S}_{\mathtt{AE}}}1dA(z)\,,\quad \text{and}\quad \boldsymbol{\pi}_{\mathtt{E}} := \frac{1}{\psi_{\mathtt{E}}}\int_{\mathcal{Z}_{\mathtt{E}}}(\mathbf{Id} - \nabla_z\boldsymbol{\chi}_{\mathtt{E}})dV\,, \qquad (244)$$

where $\boldsymbol{\chi}_{\mathtt{E}}$ solves the cell problem (231).

For the macro-scale homogeneous Neumann boundary conditions (215) –(216) we obtain thus

$$\begin{aligned}\boldsymbol{\pi}_{\mathtt{E}}\Big(M_{11}\nabla_x\mu_1^0 + M_{12}\nabla_x\mu_2^0\Big)\cdot\mathbf{n} &= 0 \qquad \text{on } \Sigma_{\mathtt{C}} \qquad (245)\\ \boldsymbol{\pi}_{\mathtt{E}}\Big(M_{12}\nabla_x\mu_1^0 + M_{22}\nabla_x\mu_2^0\Big)\cdot\mathbf{n} &= 0 \qquad \text{on } \Sigma_{\mathtt{C}} \qquad (246)\end{aligned}$$

and for the Dirichlet boundary conditions (213)

$$\begin{aligned}\frac{1}{2}(\mu_1^0 - \mu_2^0) &= \varphi_{\mathtt{E}}^{\mathsf{init}} \qquad \text{on } \Sigma_{\mathtt{E}} \qquad (247)\\ \frac{1}{2}(\mu_1^0 + \mu_2^0) &= f_{\mathtt{E}}(y_{\mathtt{E}}^{\mathsf{init}}) \qquad \text{on } \Sigma_{\mathtt{E}} \qquad (248)\end{aligned}$$

6.2.2 Application to the electrolyte:

We apply now the homogenization scheme of the previous section to the balance equations (154)–(155). Note that in the electro-neutral case, (152)–(153) is equivalent to (154)–(155), and the ε^{-2}-Order of 6.2.1 has shown that $y_{\mathtt{E}}^0$ and $\varphi_{\mathtt{E}}^0$ are indeed independent of the micro-scale variable z. When the mobility matrices $M_{\alpha\beta}$ are further independent of space, we concluded that only a single corrector $\boldsymbol{\chi}_{\mathtt{E}}$ arises, upon which in linear combinations of (152)–(153) the corrector $\boldsymbol{\pi}_{\mathtt{E}}$ simply distributive. Hence, we obtain for

$$C_h c_{\mathtt{E}} \frac{\partial y_{\mathtt{E}}}{\partial t} = \operatorname{div}\left(D_{\mathtt{E}}^y(y_{\mathtt{E}})\nabla y_{\mathtt{E}} + D_{\mathtt{E}}^\varphi(y_{\mathtt{E}})\nabla\varphi_{\mathtt{E}}\right) \qquad \mathbf{x}\in\Omega_{\mathtt{E}}^\varepsilon \tag{249}$$

$$0 = \operatorname{div}\left(S_{\mathtt{E}}(y_{\mathtt{E}})\nabla y_{\mathtt{E}} + \sigma_{\mathtt{E}}(y_{\mathtt{E}})\nabla\varphi_{\mathtt{E}}\right) \qquad \mathbf{x}\in\Omega_{\mathtt{E}}^\varepsilon\,. \tag{250}$$

with boundary conditions[12]

$$\left(D_{\mathtt{E}}^y(y_{\mathtt{E}})\nabla y_{\mathtt{E}} + D_{\mathtt{E}}^\varphi(y_{\mathtt{E}})\nabla\varphi_{\mathtt{E}}\right)\cdot\mathbf{n}_{\mathtt{E}} = -\varepsilon^1 L\cdot g(\lambda) \qquad \text{on } \Sigma_{\mathtt{AE}}^\varepsilon\,, \tag{251}$$

$$\left(S_{\mathtt{E}}(y_{\mathtt{E}})\nabla y_{\mathtt{E}} + \sigma_{\mathtt{E}}(y_{\mathtt{E}})\nabla\varphi_{\mathtt{E}}\right)\cdot\mathbf{n}_{\mathtt{E}} = -\varepsilon^1 L\cdot g(\lambda) \qquad \text{on } \Sigma_{\mathtt{AE}}^\varepsilon\,, \tag{252}$$

$$\left(D_{\mathtt{E}}^y(y_{\mathtt{E}})\nabla y_{\mathtt{E}} + D_{\mathtt{E}}^\varphi(y_{\mathtt{E}})\nabla\varphi_{\mathtt{E}}\right)\cdot\mathbf{n}_{\mathtt{E}} = 0 \qquad \text{on } \Sigma_{\mathtt{CE}}^\varepsilon\,, \tag{253}$$

$$\left(S_{\mathtt{E}}\nabla y_{\mathtt{E}}(y_{\mathtt{E}}) + \sigma_{\mathtt{E}}(y_{\mathtt{E}})\nabla\varphi_{\mathtt{E}}\right)\cdot\mathbf{n}_{\mathtt{E}} = 0 \qquad \text{on } \Sigma_{\mathtt{CE}}^\varepsilon\,, \tag{254}$$

as well as

$$\left(D_{\mathtt{E}}^y(y_{\mathtt{E}})\nabla y_{\mathtt{E}} + D_{\mathtt{E}}^\varphi(y_{\mathtt{E}})\nabla\varphi_{\mathtt{E}}\right)\cdot\mathbf{n} = 0 \qquad \text{on } \overline{\Sigma}_{\mathtt{CC}}^\varepsilon\,, \tag{255}$$

$$\left(S_{\mathtt{E}}(y_{\mathtt{E}})\nabla y_{\mathtt{E}} + \sigma_{\mathtt{E}}(y_{\mathtt{E}})\nabla\varphi_{\mathtt{E}}\right)\cdot\mathbf{n} = 0 \qquad \text{on } \overline{\Sigma}_{\mathtt{CC}}^\varepsilon\,. \tag{256}$$

and

$$\varphi_{\mathtt{E}} = \varphi_{\mathtt{E}}^{\mathsf{init}} \qquad \text{on } \Sigma_{\mathtt{EE}}^\varepsilon \tag{257}$$

$$y_{\mathtt{E}} = \varphi_{\mathtt{E}}^{\mathsf{init}} \qquad \text{on } \Sigma_{\mathtt{EE}}^\varepsilon \tag{258}$$

the leading order equations

$$C_h c_{\mathtt{E}}(y_{\mathtt{E}}^0)\frac{\partial y_{\mathtt{E}}^0}{\partial t} = \operatorname{div}_x(\boldsymbol{\pi}_{\mathtt{E}} D_{\mathtt{E}}^y(y_{\mathtt{E}}^0)\nabla_x y_{\mathtt{E}}^0 + \boldsymbol{\pi}_{\mathtt{E}} D_{\mathtt{E}}^\varphi(y_{\mathtt{E}}^0)\nabla_x\varphi_{\mathtt{E}}^0) - \frac{\theta_{\mathtt{AE}}}{\psi_{\mathtt{E}}}\fint_{\mathcal{S}_{\mathtt{AE}}} Lg(\lambda^0)dA \quad \text{on } \Omega \tag{259}$$

$$0 = \operatorname{div}_x(\boldsymbol{\pi}_{\mathtt{E}} S_{\mathtt{E}}(y_{\mathtt{E}}^0)\nabla_x y_{\mathtt{E}}^0 + \boldsymbol{\pi}_{\mathtt{E}}\sigma_{\mathtt{E}}(y_{\mathtt{E}}^0)\nabla\varphi_{\mathtt{E}}^0) - \frac{\theta_{\mathtt{AE}}}{\psi_{\mathtt{E}}}\fint_{\mathcal{S}_{\mathtt{AE}}} Lg(\lambda^0)dA \quad \text{on } \Omega \tag{260}$$

with macro-scale boundary conditions

$$(\boldsymbol{\pi}_{\mathtt{E}} D_{\mathtt{E}}^y(y_{\mathtt{E}}^0)\nabla_x y_{\mathtt{E}}^0 + \boldsymbol{\pi}_{\mathtt{E}} D_{\mathtt{E}}^\varphi(y_{\mathtt{E}}^0)\nabla_x\varphi_{\mathtt{E}}^0)\cdot\mathbf{n} = 0 \qquad \text{on } \Sigma_{\mathtt{C}} \tag{261}$$

$$(\boldsymbol{\pi}_{\mathtt{E}} S_{\mathtt{E}}(y_{\mathtt{E}}^0)\nabla_x y_{\mathtt{E}}^0 + \boldsymbol{\pi}_{\mathtt{E}}\sigma_{\mathtt{E}}(y_{\mathtt{E}}^0)\nabla\varphi_{\mathtt{E}}^0)\cdot\mathbf{n} = 0 \qquad \text{on } \Sigma_{\mathtt{C}} \tag{262}$$

$$\varphi_{\mathtt{E}}^0 = 0 \qquad \text{on } \Sigma_{\mathtt{E}} \tag{263}$$

$$y_{\mathtt{E}}^0 = y_{\mathtt{E}}^{\mathsf{init}} \qquad \text{on } \Sigma_{\mathtt{E}}\,. \tag{264}$$

[12] $\mathbf{n}$ is the outward normal vector to $\partial\Omega_{\mathtt{E}}$.

6.3 Active Phase: Expansion of (149) – (150)

Next, we discuss the active phase equations

$$C_h \frac{\partial y_{\mathtt{A}}^\varepsilon}{\partial t} = \varepsilon^2 \operatorname{div}\left(M_{\mathtt{A}}(y_{\mathtt{A}}^\varepsilon)\nabla \mu_{\mathtt{A}}^\varepsilon\right) \qquad \mathbf{x} \in \Omega_{\mathtt{A}}^\varepsilon\,, \tag{265}$$

$$\mu_{\mathtt{A}}^\varepsilon = f_{\mathtt{A}}(y_{\mathtt{A}}^\varepsilon) - \gamma_{\mathtt{A}}\varepsilon^2 \operatorname{div}\nabla y_{\mathtt{A}}^\varepsilon \qquad \mathbf{x} \in \Omega_{\mathtt{A}}\,. \tag{266}$$

For the chemical potential $\mu_{\mathtt{A}}^\varepsilon$ we obtain

$$\begin{aligned}\mu_{\mathtt{A}}^\varepsilon = f_{\mathtt{A}}(y_{\mathtt{A}}^0) + f'_{\mathtt{A}}|_{y_{\mathtt{A}}^0}\varepsilon - \Big[\operatorname{div}_z \gamma_{\mathtt{A}}\nabla_z y_{\mathtt{A}}^0\Big] \\ - \varepsilon^1\Big[\operatorname{div}_x \gamma_{\mathtt{A}}\nabla_z y_{\mathtt{A}}^0 + \operatorname{div}_z \gamma_{\mathtt{A}}\nabla_x y_{\mathtt{A}}^0 + \operatorname{div}_z \gamma_{\mathtt{A}}\nabla_z y_{\mathtt{A}}^1\Big] + \mathcal{O}(\varepsilon^2)\end{aligned} \tag{267}$$

and thus identify

$$\mu_{\mathtt{A}}^0 = f_{\mathtt{A}}(y_{\mathtt{A}}^0) - \Big[\operatorname{div}_z \gamma_{\mathtt{A}}\nabla_z y_{\mathtt{A}}^0\Big] \tag{268}$$

$$\mu_{\mathtt{A}}^1 = f'_{\mathtt{A}}|_{y_{\mathtt{A}}^0} - \varepsilon^1\Big[\operatorname{div}_x \gamma_{\mathtt{A}}\nabla_z y_{\mathtt{A}}^0 + \operatorname{div}_z \gamma_{\mathtt{A}}\nabla_x y_{\mathtt{A}}^0 + \operatorname{div}_z \gamma_{\mathtt{A}}\nabla_z y_{\mathtt{A}}^1\Big]\,. \tag{269}$$

For (265) we obtain

$$\varepsilon^2 \operatorname{div}\left(M_{\mathtt{A}}(y_{\mathtt{A}}^\varepsilon)\nabla \mu_{\mathtt{A}}^\varepsilon\right) = \varepsilon^0\Big[\operatorname{div}_z M_{\mathtt{A}}(y_{\mathtt{A}}^0)\nabla_z \mu_{\mathtt{A}}^0\Big] + \mathcal{O}(\varepsilon) \tag{270}$$

and thus in leading order

$$C_h \frac{\partial y_{\mathtt{A}}^0}{\partial t} = \operatorname{div}_z M_{\mathtt{A}}(y_{\mathtt{A}}^0)\nabla_z \mu_{\mathtt{A}}^0 \qquad \text{on } \Omega \times \mathcal{Z}_{\mathtt{A}} \tag{271}$$

$$\mu_{\mathtt{A}}^0 = f_{\mathtt{A}}(y_{\mathtt{A}}^0) - \operatorname{div}_z \gamma_{\mathtt{A}}\nabla_z y_{\mathtt{A}}^0 \qquad \text{on } \Omega \times \mathcal{Z}_{\mathtt{A}} \tag{272}$$

together with the boundary conditions

$$(\gamma_{\mathtt{A}}\nabla_z y_{\mathtt{A}}^0)\cdot \mathbf{n} = 0 \qquad \text{on } \Omega \times \mathcal{S}_{\mathtt{AE}}, \tag{273}$$

$$(M_{\mathtt{A}}(y_{\mathtt{A}}^0)\nabla_z \mu_{\mathtt{A}}^0)\cdot \mathbf{n} = L \cdot g(\lambda^0) \qquad \text{on } \Omega \times \mathcal{S}_{\mathtt{AE}}, \tag{274}$$

and

$$\lambda^0 = -\big(\varphi_{\mathtt{S}}^0 - \varphi_{\mathtt{E}}^0 + \mu_{\mathtt{A}}^0|_{\mathcal{S}_{\mathtt{AE}}} - f_{\mathtt{E}}(y_{\mathtt{E}}^0)\big)\,. \tag{275}$$

7 Summary and Outlook

In this paper, we established a unified multi-scale modeling framework for porous intercalation electrodes by systematically upscaling microscopically resolved transport and reaction equations. The resulting homogenized model provides a consistent description of ionic transport in the electrolyte, electronic conduction in the solid phase, and diffusion-driven intercalation dynamics within active particles, all embedded within a thermodynamically consistent formulation.

A distinguishing aspect of the derived framework is its ability to represent phase separation phenomena at the electrode scale. This is achieved through the use of general multi-well free energy functions for intercalated cations, combined with gradient-based regularization terms that account for interfacial

energetic effects. The homogenization procedure demonstrates how particle-scale phase-transition mechanisms are transferred to the macroscopic balance equations without *ad hoc* closure assumptions, thereby extending classical porous-electrode models beyond monotone constitutive behavior.

The homogenized equations naturally give rise to a coupled macroscopic–microscopic structure, in which lithium diffusion within individual particles remains fully resolved and enters the macroscopic problem through nonlocal source terms. This coupling introduces intrinsic memory effects and time delays in the electrode response, which are absent in reduced single-scale descriptions. Despite this increased structural complexity, the model retains a dissipative evolution structure and admits a formulation as a coupled system of parabolic and elliptic equations.

Overall, this work provides the theoretical foundation for a new class of DFN-type porous-electrode models that remain valid in the presence of multiple phase transitions. By focusing on a general constitutive formulation and a systematic upscaling procedure, the framework is designed to serve as a flexible basis for numerical simulation, analysis, and application to a broad range of intercalation materials.

The resulting single-electrode model consists of four coupled partial differential equations. Despite this apparent complexity, the system remains comparatively simple in the sense that it is fully closed and does not require additional ad hoc modeling assumptions or external closure relations.

7.1 Summary of the homogenized balance equations

We summarize here the derived model for a porous intercalation electrode that can undergo multiple phase transitions upon cation intercalation. Note that we drop here the ^{0} syntax for the leading order terms as well as the $\hat{\cdot}$ syntax for all non-dimensionalized quantities (c.f. table 1). On the macro-scale, we obtained the following set of non-dimensionalized balance equations, which hold for arbitrary geometries $\Omega \subset \mathbb{R}^3$, i.e.

$$C_h c_{\mathtt{E}}(y_{\mathtt{E}})\frac{\partial y_{\mathtt{E}}}{\partial t} = \operatorname{div}_x(\boldsymbol{\pi}_{\mathtt{E}} D_{\mathtt{E}}^y(y_{\mathtt{E}})\nabla_x y_{\mathtt{E}} + \boldsymbol{\pi}_{\mathtt{E}} D_{\mathtt{E}}^{\varphi}(y_{\mathtt{E}})\nabla_x \varphi_{\mathtt{E}}) - \frac{\theta_{\mathtt{AE}}}{\psi_{\mathtt{E}}} \fint_{\mathcal{S}_{\mathtt{AE}}} L g(\lambda) dA \quad \text{on } \Omega \tag{276}$$

$$0 = \operatorname{div}_x(\boldsymbol{\pi}_{\mathtt{E}} S_{\mathtt{E}}(y_{\mathtt{E}})\nabla_x y_{\mathtt{E}} + \boldsymbol{\pi}_{\mathtt{E}} \sigma_{\mathtt{E}}(y_{\mathtt{E}})\nabla \varphi_{\mathtt{E}}) - \frac{\theta_{\mathtt{AE}}}{\psi_{\mathtt{E}}} \fint_{\mathcal{S}_{\mathtt{AE}}} L g(\lambda) dA \quad \text{on } \Omega \tag{277}$$

$$0 = \operatorname{div}_x\big(\boldsymbol{\pi}_{\mathtt{S}} \sigma_{\mathtt{S}} \nabla_x \varphi_{\mathtt{S}}\big) + \frac{\theta_{\mathtt{AE}}}{\psi_{\mathtt{A}}} \fint_{\mathcal{S}_{\mathtt{AE}}} L\, g(\lambda) dA(z) \quad \text{on } \Omega \tag{278}$$

with

$$\lambda = -\big(\varphi_{\mathtt{S}} - \varphi_{\mathtt{E}} + \mu_{\mathtt{A}}|_{\mathcal{S}_{\mathtt{AE}}} - f_{\mathtt{E}}(y_{\mathtt{E}})\big) \quad \text{on } \Omega \times \mathcal{S}_{\mathtt{AE}} \tag{279}$$

and macro-scale boundary conditions

$$(\boldsymbol{\pi}_{\mathtt{E}} D_{\mathtt{E}}^y(y_{\mathtt{E}})\nabla_x y_{\mathtt{E}} + \boldsymbol{\pi}_{\mathtt{E}} D_{\mathtt{E}}^{\varphi}(y_{\mathtt{E}})\nabla_x \varphi_{\mathtt{E}}) \cdot \mathbf{n} = 0 \quad \text{on } \Sigma_{\mathtt{C}} \tag{280}$$

$$(\boldsymbol{\pi}_{\mathtt{E}} S_{\mathtt{E}}(y_{\mathtt{E}})\nabla_x y_{\mathtt{E}} + \boldsymbol{\pi}_{\mathtt{E}} \sigma_{\mathtt{E}}(y_{\mathtt{E}})\nabla \varphi_{\mathtt{E}}) \cdot \mathbf{n} = 0 \quad \text{on } \Sigma_{\mathtt{C}} \tag{281}$$

$$\varphi_{\mathtt{E}} = 0 \quad \text{on } \Sigma_{\mathtt{E}} \tag{282}$$

$$y_{\mathtt{E}} = y_{\mathtt{E}}^{\mathsf{init}} \quad \text{on } \Sigma_{\mathtt{E}} \tag{283}$$

$$\sigma_{\mathtt{S}} \boldsymbol{\pi}_{\mathtt{S}} \nabla_x \varphi_{\mathtt{S}}(x) \cdot \mathbf{n} = i(t) C_h \quad \text{on } \Sigma_{\mathtt{C}} \tag{284}$$

$$\sigma_{\mathtt{S}} \boldsymbol{\pi}_{\mathtt{S}} \nabla_x \varphi_{\mathtt{S}}(x) \cdot \mathbf{n} = 0 \quad \text{on } \Sigma_{\mathtt{E}}\,. \tag{285}$$

The porous media parameters [13] are the electrolyte phase fraction $\psi_{\$}$ and active phase fraction $\psi_{\mathtt{A}}$, the solid phase conductivity corrector $\boldsymbol{\pi}_{\mathtt{S}}$, the electrolyte diffusional corrector $\boldsymbol{\pi}_{\mathtt{E}}$, and the specific interfacial area $\theta_{\mathtt{AE}}$, which are computed as

$$\psi_{\mathtt{A}} := \int_{\mathcal{Z}_{\mathtt{A}}} 1 dV(z) \ , \ \boldsymbol{\pi}_{\mathtt{S}} := \frac{1}{\psi_{\mathtt{A}}} \int_{\mathcal{Z}_{\mathtt{S}}} \eta_{\mathtt{S}}(z)(\mathbf{Id} - \nabla_z \boldsymbol{\chi}_{\mathtt{S}})\, dV(z) \ , \ \theta_{\mathtt{AE}} := \int_{\mathcal{S}_{\mathtt{AE}}} 1\, dA(z) \tag{286}$$

and

$$\psi_{\mathtt{E}} := \int_{\mathcal{Z}_{\mathtt{E}}} 1 dV(z) \ , \quad \boldsymbol{\pi}_{\mathtt{E}} := \frac{1}{\psi_{\mathtt{E}}} \int_{\mathcal{Z}_{\mathtt{E}}} (\mathbf{Id} - \nabla_z \boldsymbol{\chi}_{\mathtt{E}}) dV \ , \tag{287}$$

For the active phase, we have the coupled, non-dimensionalized macro-micro scale problem on $\Omega \times \mathcal{Z}_{\mathtt{A}}$, which holds for arbitrary periodic micro-structures $\mathcal{Z}_{\mathtt{A}} \subset [0,1]^3$, yielding

$$C_h \frac{\partial y_{\mathtt{A}}}{\partial t} = \operatorname{div}_z M_{\mathtt{A}}(y_{\mathtt{A}}) \nabla_z \mu_{\mathtt{A}} \qquad \text{on } \Omega \times \mathcal{Z}_{\mathtt{A}} \tag{288}$$

$$\mu_{\mathtt{A}} = f_{\mathtt{A}}(y_{\mathtt{A}}) - \operatorname{div}_z \gamma_{\mathtt{A}} \nabla_z y_{\mathtt{A}} \qquad \text{on } \Omega \times \mathcal{Z}_{\mathtt{A}} \tag{289}$$

together with the boundary conditions

$$(\gamma_{\mathtt{A}} \nabla_z y_{\mathtt{A}}) \cdot \mathbf{n} = 0 \qquad \text{on } \Omega \times \mathcal{S}_{\mathtt{AE}}, \tag{290}$$

$$(M_{\mathtt{A}}(y_{\mathtt{A}}) \nabla_z \mu_{\mathtt{A}}) \cdot \mathbf{n} = L \cdot g(\lambda) \qquad \text{on } \Omega \times \mathcal{S}_{\mathtt{AE}}. \tag{291}$$

7.2 Outlook

Our work on the modeling, homogenization, simulation and validation of porous electrodes that can undergo multiple phase transitions spreads in three parts, where this work (Part I) is entirely devoted to the model derivation and homogenization.

Part II of this series will focus on the numerical treatment and simulation of the homogenized model derived in the present work. For Part II, we will assume spherical symmetry on the micro-scale and a 1D approximation on the macro-scale, yielding a 1D+1D-type equation system that can be considered as the thermodynamically consistent extension of the DFN-model for phase separating materials. Particular emphasis will be placed on numerical schemes that respect the underlying thermodynamic structure of the model, thereby ensuring stability and robustness even in the presence of strong nonlinearities induced by multi-well free energy functions and phase separation. The separation between electrolyte modeling and active material modeling inherent in the present formulation facilitates the transfer of independently calibrated material parameters.

Based on these discretization strategies, Part II will investigate transient charge and discharge processes under finite C-rate conditions. Special attention will be paid to the emergence and evolution of phase boundaries, either within or among particles, and their impact on macroscopic observables such as voltage curves and subsequently hysteretic effects . These studies will demonstrate how the additional micro-structural resolution provided by the present framework extends classical DFN-type models and enables a more accurate description of non-equilibrium cycling behavior. For higher C-rates, we discuss how the coupled micro–macro structure of the model naturally leads to a phase separations within the particles (i.e. on the micro-scale), competing with concentration gradients due to diffusional effects as well as the macroscopic phase separation among the particles. We perform numerical simulations to analyze the interplay between diffusion-limited transport inside active particles,

[13] Note that we set vol$\{\mathcal{Z}\} = 1$.

electrolyte transport, and interfacial reaction kinetics. Special attention will be paid to the emergence and evolution of phase boundaries, either within or among particles, and their impact on macroscopic observables such as voltage curves and subsequently hysteretic effects These studies will demonstrate how the additional micro-structural resolution provided by the present framework extends classical DFN-type models and enables a more accurate description of non-equilibrium cycling behavior.

Part III will be devoted to the analysis of open-circuit voltage conditions, equilibrium states, and model validation. In this context, the multi-well free energy formulation allows for a direct and thermodynamically consistent connection between microscopic phase equilibria in the active material and macroscopic voltage characteristics. Part III will analyze the OCV solutions of the homogenized model and investigate how phase coexistence at the particle level manifests itself in voltage plateaus and hysteresis effects at the electrode scale. We will discuss on a sound mathematical basis how the hysteresis of the cell voltage is *encoded* in the spatial structure of the concentration field $y_{\mathtt{A}}$, and why spatially constant solutions that arise in simple diffusion equations cannot be considered as valid solutions in the context of phase separating materials. In part III of this series, we will also use two different approaches to derive a model for very slow charging of the battery, i.e. OCV conditions. This can be done either emerging from our current 3D+3D model or ad hoc from the microscopic model. We will see how the function $f_{\mathtt{A}}$ transforms under these conditions to an effective $\bar{f}_{\mathtt{A}}$ and we will be able to provide explicit formulas for this $\bar{f}_{\mathtt{A}}$, yielding a forward-backward parabolic equation. Furthermore, Part III will address parameter identification and validation of the proposed framework against experimental data. Experimental OCV curves and equilibrium measurements will be used to assess the predictive capabilities of the model and to identify the role of interfacial energy contributions and particle-scale phase separation. Together, these investigations will establish the proposed framework as a predictive and extensible modeling tool for porous intercalation electrodes operating across a wide range of regimes.

References

[1] A. Bonnefont, F. Argoul, M. Bazant. “Analysis of Diffuse-Layer Effects on Time-Dependent Interfacial Kinetics”. In: *J. Electroanal. Chem.* 500.1-2 (2001), pp. 52–61.

[2] P. Bai, D. A. Cogswell, and M. Z. Bazant. “Suppression of Phase Separation in LiFePO4 Nanoparticles During Battery Discharge”. In: *Nano Letters* 11.11 (2011), pp. 4890–4896.

[3] M. Z. Bazant. “Theory of Chemical Kinetics and Charge Transfer based on Nonequilibrium Thermodynamics”. In: *Accounts of Chemical Research* 46.5 (2013), pp. 1144–1160.

[4] M. Z. Bazant, K. T. Chu, and B. J. Bayly. “Current-Voltage Relations for Electrochemical Thin Films”. In: *SIAM J. Appl. Math.* 65.5 (2005), pp. 1463–1484.

[5] P. Biesheuvel, M. van Soestbergen, and M. Bazant. “Imposed currents in galvanic cells”. In: *Electrochim. Acta* 54.21 (2009), pp. 4857–4871.

[6] F. Brosa Planella et al. “A continuum of physics-based lithium-ion battery models reviewed”. In: *Progress in Energy* 4.4 (2022), p. 042003.

[7] F. Brosa Planella, M. Sheikh, and W. D. Widanage. “Systematic derivation and validation of a reduced thermal-electrochemical model for lithium-ion batteries using asymptotic methods”. In: *Electrochimica Acta* 388 (2021), p. 138524.

[8] J. W. Cahn. “Free Energy of a Nonuniform System. II. Thermodynamic Basis”. In: *J. Chem. Phys.* 30.5 (1959), pp. 1121–1124.

[9] J. W. Cahn and J. E. Hilliard. “Free Energy of a Nonuniform System. I. Interfacial Free Energy”. In: *J. Chem. Phys.* 28.2 (1958), pp. 258–267.

[10] K. Chu and M. Bazant. “Nonlinear Electrochemical Relaxation around Conductors”. In: *Physical Review E* 74.1 (2006), p. 011501.

[11] F. Ciucci and W. Lai. “Derivation of Micro/Macro Lithium Battery Models from Homogenization”. In: *Transport in Porous Media* 88.2 (2011), pp. 249–270.

[12] D. A. Cogswell and M. Z. Bazant. “Coherency Strain and the Kinetics of Phase Separation in LiFePO4 Nanoparticles”. In: *ACS Nano* 6.3 (2012), pp. 2215–2225.

[13] R. Defay, I. Prigogine, and A. Sanfeld. “Surface thermodynamics”. In: *Journal of Colloid and Interface Science* 58.3 (1977), pp. 498–510.

[14] W. Dreyer, C. Guhlke, and M. Landstorfer. “A mixture theory of electrolytes containing solvation effects”. In: *Electrochemistry Communications* 43.0 (2014), pp. 75–78.

[15] W. Dreyer et al. “New insights on the interfacial tension of electrochemical interfaces and the Lippmann equation”. In: *European Journal of Applied Mathematics* 29.4 (2018), pp. 708–753.

[16] W. Dreyer et al. “Phase transition in a rechargeable lithium battery”. In: *European J. Appl. Math.* 22.03 (2011), pp. 267–290.

[17] W. Dreyer et al. “The Thermodynamic Origin of Hysteresis in Insertion Batteries”. In: *Nature Mater.* 9.5 (2010), pp. 448–453.

[18] W. Dreyer, C. Guhlke, and R. Huth. “The behavior of a many-particle electrode in a lithium-ion battery”. In: *Physica D* 240.12 (2011), pp. 1008–1019.

[19] W. Dreyer, C. Guhlke, and R. Muller. “A new perspective on the electron transfer: recovering the Butler-Volmer equation in non-equilibrium thermodynamics”. In: *Phys. Chem. Chem. Phys.* 18 (2016), pp. 24966–24983.

[20] W. Dreyer, C. Guhlke, and R. Muller. “Modeling of electrochemical double layers in thermodynamic non-equilibrium”. In: *Phys. Chem. Chem. Phys.* 17 (2015), pp. 27176–27194.

[21] W. Dreyer, C. Guhlke, and R. Muller. “Overcoming the shortcomings of the Nernst-Planck model”. In: *Phys. Chem. Chem. Phys.* 15 (2013), pp. 7075–7086.

[22] W. Dreyer, C. Guhlke, and R. Müller. “Bulk-Surface Electrothermodynamics and Applications to Electrochemistry”. In: *Entropy* 20.12 (2018), p. 939.

[23] T. R. Ferguson and M. Z. Bazant. “Nonequilibrium Thermodynamics of Porous Electrodes”. In: *Journal of The Electrochemical Society* 159.12 (2012), A1967–A1985.

[24] R. Garcia, C. Bishop, and W. Carter. “Thermodynamically Consistent Variational Principles with Applications to Electrically and Magnetically Active Systems”. In: *Acta Mater.* 52.1 (2004), pp. 11–21.

[25] S. de Groot and P. Mazur. *Non-Equilibrium Thermodynamics*. 1984.

[26] C. Guhlke. “Theorie der elektrochemischen Grenzfläche”. PhD thesis. 2015.

[27] M. Heida, M. Landstorfer, and M. Liero. “Homogenization of a Porous Intercalation Electrode with Phase Separation”. In: *Multiscale Modeling & Simulation* 22.3 (2024), pp. 1068–1096.

[28] J. Maier. *Physical Chemistry of Ionic Materials*. 2004.

[29] J. Newman, K. Thomas. *Electrochemical Systems*. 2014.

[30] J. Newman, K. Thomas, H. Hafezi D. Wheeler. “Modeling of Lithium-Ion Batteries”. In: *J. Power Sources* 119 (2003), pp. 838–843.

[31] J. Newman, W. Tiedemann. “Porous-Electrode Theory with Battery Applications”. In: *Aiche J.* 21 (1975), pp. 25–41.

[32] M. Landstorfer, C. Guhlke, and W. Dreyer. “Theory and structure of the metal-electrolyte interface incorporating adsorption and solvation effects”. In: *Electrochimica Acta* 201 (2016), pp. 187–219.

[33] M. Landstorfer et al. “A modelling framework for efficient reduced order simulations of parametrised lithium-ion battery cells”. In: *European Journal of Applied Mathematics* 34.3 (2023), pp. 554–591.

[34] M. Landstorfer. “A Discussion of the Cell Voltage during Discharge of an Intercalation Electrode for Various C-Rates Based on Non-Equilibrium Thermodynamics and Numerical Simulations”. In: *Journal of The Electrochemical Society* 167.1 (2019), p. 013518.

[35] M. Landstorfer. “Boundary Conditions for Electrochemical Interfaces”. In: *Journal of The Electrochemical Society* 164.11 (2017), E3671–E3685.

[36] M. Landstorfer, S. Funken, and T. Jacob. “An advanced model framework for solid electrolyte intercalation batteries”. In: *Phys. Chem. Chem. Phys.* 13 (2011), pp. 12817–12825.

[37] M. Landstorfer and T. Jacob. “Mathematical modeling of intercalation batteries at the cell level and beyond”. In: *Chem. Soc. Rev.* 42 (2013), pp. 3234–3252.

[38] M. Landstorfer, B. Prifling, and V. Schmidt. “Mesh generation for periodic 3D microstructure models and computation of effective properties”. In: *Journal of Computational Physics* 431 (2021), p. 110071.

[39] A. Latz and J. Zausch. “Thermodynamic derivation of a Butler–Volmer model for intercalation in Li-ion batteries”. In: *Electrochimica Acta* 110 (2013), pp. 358–362.

[40] M. Doyle, T. Fuller, J. Newman. “Modeling of Galvanostatic Charge and Discharge of the Lithium / Polymer / Insertion Cell”. In: *J. Electrochem. Soc.* 140.6 (1993), pp. 1526–1533.

[41] I. Müller. *Thermodynamics*. 1985.

[42] R. Müller and M. Landstorfer. “Galilean Bulk-Surface Electrothermodynamics and Applications to Electrochemistry”. In: *Entropy* 25.3 (2023).

[43] J. Newman. “The Polarized Diffuse Double Layer”. In: *Transactions of the Faraday Society* (1965).

[44] A. Sanfeld. *Introduction to the thermodynamics of charged and polarized layers*. 1968.

[45] T. Fuller, M. Doyle, J. Newman. “Simulation and Optimization of the Dual Lithium Ion Insertion Cell”. In: *J. Electrochem. Soc.* 141 (1994), pp. 1–9.

[46] S. Whitaker. *The method of volume averaging*. 1999.

A Cross-Correctors

The order ε^{-1} problem reads with $\nabla_z \mu_1^0 = 0$ and $\nabla_z \mu_2^0 = 0$

$$\operatorname{div}_z(M_{11}\nabla_z \mu_1^1 + M_{12}\nabla_z \mu_2^1 + M_{11}\nabla_x \mu_1^0 + M_{12}\nabla_x \mu_2^0) = 0 \tag{292}$$

$$\operatorname{div}_z(M_{12}\nabla_z \mu_1^1 + M_{22}\nabla_z \mu_2^1 + M_{12}\nabla_x \mu_1^0 + M_{22}\nabla_x \mu_2^0) = 0 \tag{293}$$

with boundary conditions

$$(M_{11}\nabla_z\mu_1^1 + M_{12}\nabla_z\mu_2^1 + M_{11}\nabla_x\mu_1^0 + M_{12}\nabla_x\mu_2^0)\cdot\mathbf{n} = 0 \tag{294}$$
$$(M_{12}\nabla_z\mu_1^1 + M_{22}\nabla_z\mu_2^1 + M_{12}\nabla_x\mu_1^0 + M_{22}\nabla_x\mu_2^0)\cdot\mathbf{n} = 0\,. \tag{295}$$

We expect

$$\mu_1^1 = -\boldsymbol{\chi}_{11}\nabla_x\mu_1^0 - \boldsymbol{\chi}_{12}\nabla_x\mu_2^0 \tag{296}$$
$$\mu_2^1 = -\boldsymbol{\chi}_{21}\nabla_x\mu_1^0 - \boldsymbol{\chi}_{22}\nabla_x\mu_2^0\,, \tag{297}$$

i.e. a micro-scale intercation beteween μ_1^0 and μ_2^0 propagating into μ_1^1 and μ_2^1.

Insertion yields

$$\mathrm{div}_z((M_{11} - M_{11}\nabla_z\boldsymbol{\chi}_{11} - M_{12}\nabla_z\boldsymbol{\chi}_{21})\nabla_x\mu_1^0 + (M_{12} - M_{11}\nabla_z\boldsymbol{\chi}_{12} - M_{12}\nabla_z\boldsymbol{\chi}_{22})\nabla_x\mu_2^0) = 0 \tag{298}$$
$$\mathrm{div}_z((M_{12} - M_{12}\nabla_z\boldsymbol{\chi}_{11} - M_{22}\nabla_z\boldsymbol{\chi}_{21})\nabla_x\mu_1^0 + (M_{22} - M_{12}\nabla_z\boldsymbol{\chi}_{12} - M_{22}\nabla_z\boldsymbol{\chi}_{22})\nabla_x\mu_2^0) = 0 \tag{299}$$

and for the boundary conditions

$$((M_{11} - M_{11}\nabla_z\boldsymbol{\chi}_{11} - M_{12}\nabla_z\boldsymbol{\chi}_{21})\nabla_x\mu_1^0 + (M_{12} - M_{11}\nabla_z\boldsymbol{\chi}_{12} - M_{12}\nabla_z\boldsymbol{\chi}_{22})\nabla_x\mu_2^0)\cdot\mathbf{n} = 0 \tag{300}$$
$$((M_{12} - M_{12}\nabla_z\boldsymbol{\chi}_{11} - M_{22}\nabla_z\boldsymbol{\chi}_{21})\nabla_x\mu_1^0 + (M_{22} - M_{12}\nabla_z\boldsymbol{\chi}_{12} - M_{22}\nabla_z\boldsymbol{\chi}_{22})\nabla_x\mu_2^0)\cdot\mathbf{n} = 0 \tag{301}$$

Hence, we expect

$$\mathrm{div}_z((M_{11}\mathbf{Id} - M_{11}\nabla_z\boldsymbol{\chi}_{11} - M_{12}\nabla_z\boldsymbol{\chi}_{21})) = 0 \tag{302}$$
$$\mathrm{div}_z((M_{12}\mathbf{Id} - M_{11}\nabla_z\boldsymbol{\chi}_{12} - M_{12}\nabla_z\boldsymbol{\chi}_{22})) = 0 \tag{303}$$
$$\mathrm{div}_z((M_{12}\mathbf{Id} - M_{12}\nabla_z\boldsymbol{\chi}_{11} - M_{22}\nabla_z\boldsymbol{\chi}_{21})) = 0 \tag{304}$$
$$\mathrm{div}_z((M_{22}\mathbf{Id} - M_{12}\nabla_z\boldsymbol{\chi}_{12} - M_{22}\nabla_z\boldsymbol{\chi}_{22})) = 0 \tag{305}$$

since (298) and (299) hold for every combination of $(\nabla_x\mu_1^0, \nabla_x\mu_2^0)$.

Note, **if** $\boldsymbol{\chi}_{12} = \boldsymbol{\chi}_{21}$ we can conclude

$$\mathrm{div}_z((M_{11} - M_{22})\nabla_z\boldsymbol{\chi}_{12} + M_{12}\nabla_z(\boldsymbol{\chi}_{22} - \boldsymbol{\chi}_{11})) = 0 \tag{306}$$
$$((M_{11} - M_{22})\nabla_z\boldsymbol{\chi}_{12} + M_{12}\nabla_z(\boldsymbol{\chi}_{22} - \boldsymbol{\chi}_{11}))\cdot\mathbf{n} = 0 \tag{307}$$

whereby

$$\nabla_z\boldsymbol{\chi}_{12} = \frac{M_{12}}{(M_{11} - M_{22})}\nabla_z(\boldsymbol{\chi}_{11} - \boldsymbol{\chi}_{22}) \qquad \textbf{if} \qquad M_{11} \neq M_{22} \tag{308}$$

Note that this entails $\boldsymbol{\chi}_{12} = 0$ if $M_{12} = 0$. Further, if $M_{11} = M_{22}$ we obtain $\boldsymbol{\chi}_{22} = \boldsymbol{\chi}_{11}$.

We proceed with $M_{11} \neq M_{22}$ and have

$$\operatorname{div}_z(\mathbf{Id} - \nabla_z \boldsymbol{\chi}_{11} - \frac{M_{12}^2}{M_{11}(M_{11}-M_{22})}\nabla_z(\boldsymbol{\chi}_{11}-\boldsymbol{\chi}_{22}) = 0 \tag{309}$$

$$\operatorname{div}_z(\mathbf{Id} - \nabla_z \boldsymbol{\chi}_{22} - \frac{M_{12}^2}{M_{22}(M_{11}-M_{22})}\nabla_z(\boldsymbol{\chi}_{11}-\boldsymbol{\chi}_{22}) = 0 \tag{310}$$

whereby we can write

$$\nabla_z \boldsymbol{\chi}_{11} = \Big(\mathbf{Id} + \frac{M_{12}^2}{M_{11}(M_{11}-M_{22})}\nabla_z \boldsymbol{\chi}_{22}\Big)\big(\frac{M_{11}(M_{11}-M_{22})+M_{12}^2}{M_{11}(M_{11}-M_{22})}\big)^{-1} \tag{311}$$

$$\tag{312}$$

Reinsertion into (310) equation gives

$$(\mathbf{Id} - \nabla_z \boldsymbol{\chi}_{22} + \frac{M_{12}^2}{M_{22}(M_{11}-M_{22})}\nabla_z \boldsymbol{\chi}_{22}) - \frac{M_{12}^2}{M_{22}(M_{11}-M_{22})}\nabla_z \boldsymbol{\chi}_{11} \tag{313}$$

$$= A \cdot (\mathbf{Id} - \nabla_z \boldsymbol{\chi}_{22}) \tag{314}$$

with

$$A := \frac{M_{11}^2 M_{22} - M_{11}M_{22}^2 - M_{11}M_{12}^2 + M_{22}M_{12}^2}{M_{22}\,(M_{11}^2 - M_{11}M_{22} + M_{12}^2)} \tag{315}$$

Since A is constant w.r.t. z (but dependent on u_i^0) we can actually deduce

$$\operatorname{div}(\mathbf{Id} - \nabla \boldsymbol{\chi}_{22}) = 0 \tag{316}$$

$$(\mathbf{Id} - \nabla \boldsymbol{\chi}_{22}) \cdot \mathbf{n} = 0 \tag{317}$$

to determine $\boldsymbol{\chi}_{22}$.

In eq. (310) we can exploit $\operatorname{div}_z(\mathbf{Id} - \nabla_z \boldsymbol{\chi}_{22}) = 0$ to obtain

$$\operatorname{div}_z\Big(\frac{M_{12}^2}{M_{22}(M_{11}-M_{22})}\nabla_z(\boldsymbol{\chi}_{11}-\boldsymbol{\chi}_{22})\Big) = 0 \tag{318}$$

which finally yields

$$\nabla_z \boldsymbol{\chi}_{11} = \nabla_z \boldsymbol{\chi}_{22}\,. \tag{319}$$

and thus

$$\boldsymbol{\chi}_{11} = \boldsymbol{\chi}_{22} =: \boldsymbol{\chi}_{\mathrm{E}} \tag{320}$$

as well as

$$\boldsymbol{\chi}_{12} = \mathbf{0}\,. \tag{321}$$